Lab on a Chip

CRITICAL REVIEW

View Article Online
View Journal | View Issue

Cite this: *Lab Chip*, 2026, **26**, 1444

Wearable biosensors for disease diagnostics and health monitoring: recent progress and emerging technologies

Zixuan Ren and Yue Cui *

Wearable biosensors leverage microfluidic technology for precise biofluid sampling and directional transport, and utilize electrical or optical sensing mechanisms for reliable detection of target physiological parameters. By synergizing microfluidics and sensing technologies, these devices provide innovative solutions for biomarker monitoring, demonstrating broad potential in health tracking and chronic disease management. With ongoing advances in smart materials, multiplex detection capabilities, and artificial intelligence-driven technologies, wearable biosensors are evolving into cornerstone tools for telemedicine and precision diagnostics. This work reviews recent progress in microfluidic-integrated wearable biosensors for disease diagnostics and health monitoring. We systematically examine sensing approaches for different analytes based on their biological characteristics, covering three key categories: (1) metabolite sensing, including microneedle-based detection, noninvasive optical/electrical methods, multimodal platforms, and closed-loop diabetes management systems; (2) protein sensing, encompassing both label-free and labeled electrical/optical techniques; and (3) nucleic acid sensing, which involves sampling protocols, amplification strategies, and label-free detection approaches. The review highlights the interaction between biomarker biological characteristics, sensing strategies, and microfluidic approaches in the development of wearable biosensing platforms, and is expected to guide the development of next-generation intelligent disease diagnostics and health monitoring devices.

Received 18th September 2025,
Accepted 5th January 2026

DOI: 10.1039/d5lc00892a

rsc.li/loc

Introduction

Wearable biosensors are miniature, flexible devices that rapidly and sensitively detect disease biomarkers by converting biochemical recognition events into optical or electrical signals. These devices are reshaping the way diseases are monitored and diagnosed. With advances in manufacturing technologies, the emergence of high-performance materials, and the deep integration of artificial intelligence, diagnostic technologies are experiencing unprecedented development opportunities—among which innovations in wearable biosensor technology stand out. Leveraging advantages such as miniaturization, flexibility, real-time data acquisition, and non-invasive detection, wearable sensors enable early diagnosis of potential diseases and continuous monitoring of disease progression, thereby expanding their applications in the healthcare sector.[1–3]

Metabolites, proteins, and nucleic acids are critical biomarkers for a variety of diseases, and all are playing significant roles in disease monitoring and diagnostics. First, metabolites are the direct products of cellular metabolic processes and provide real-time insights into the physical or psychiatric condition. Due to their dynamic concentration changes with time, metabolites are ideal for continuous monitoring.[4] Common metabolites include glucose,[5] lactate,[6] and uric acid (UA).[7] Glucose is a key indicator for diabetes management and wearable continuous glucose monitors (CGM) are widely used clinically.[8] Lactate is usually associated with hypoxia, sepsis, and shock.[9] Elevated UA levels may reflect metabolic syndrome.[10] Second, proteins usually serve as highly specific disease indicators and are often involved in pathological processes, immune responses, and inflammation. For example, C-reactive protein (CRP) reflects inflammatory states and is used in evaluating infection, or chronic inflammation.[11] Cytokines, such as interleukin-6 (IL-6) and tumour necrosis factor-α (TNF-α), are key indicators in autoimmune diseases and cancer-related immune responses.[12] Third, nucleic acids including DNA, RNA, and micro-RNA (miRNA) offer an ideal tool for early detection and stratification of diseases.[13] For instance, miRNA-21 is usually overexpressed in various types of cancer; SARS-CoV-2 RNA detection is the gold standard for COVID-19 diagnosis.[14] Therefore, incorporating the biosensing detection of metabolites, proteins, and nucleic acids into wearable platforms allows for the comprehensive monitoring

School of Materials Science and Engineering, State Key Laboratory of Vascular and Homeostasis and Remodeling, Peking University, Beijing 100871, P.R. China.
E-mail: ycui@pku.edu.cn

and management of multiple diseases, promoting personalized and preventative healthcare.[15,16]

To more effectively analyze, detect, and monitor these biomarkers, wearable biosensors sample a variety of biofluids, including sweat,[17–19] interstitial fluid,[20–22] saliva,[23–25] tears,[26–28] and exhaled breath.[29,30] For these biofluids, common sampling methods mainly include spontaneous excretion,[31] reverse iontophoresis,[32] vacuum suction,[33] microneedle-based extraction,[34] and stimulation-induced sampling.[35] By enabling non-invasive or minimally-invasive sampling, they allow for the analysis of macromolecules (*e.g.*, proteins and nucleic acids),[29,36–38] metabolites (*e.g.*, glucose, lactate, and uric acid),[33,39–41] and hormones (*e.g.*, cortisol).[23,42–44] Common electrical sensing devices include electrochemical methods,[45,46] flexible capacitors,[47,48] and field effect transistor (FET)-based biosensors,[49] which offer advantages such as ease of integration, low cost, and high accuracy, though improvements in long-term stability are still needed. Colorimetric sensing (*e.g.*, paper-based assays) is simple and cost-effective but generally limited in sensitivity.[50–53] Other optical detection methods (*e.g.*, fluorescence,[54–56] surface-enhanced Raman,[57,58] and chemiluminescence[59,60]) provide high sensitivity and strong resistance to interference but may depend on external light sources or complex detection modules.[20,61] The choice of sensing strategy should be tailored to the target analyte. High concentration analytes such as CRP can utilize colorimetric approaches,[50,55] while the detection of low concentration inflammatory markers (*e.g.*, IL-6, TNF-α) benefits more from highly sensitive optical techniques such as fluorescence.[62,63]

The integration of microfluidic technology has significantly promoted the development of wearable biosensors by providing precise control over biofluid sampling, transport, and reaction processes.[64,65] Structural designs employing capillary forces, wettability, and hydrophobic valves enable time-sequenced flow routing, automatic fluid triggering, and reagent activation without external power. Meanwhile, active microfluidic elements such as micropumps, electroosmotic flow units, and iontophoretic patches enhance fluid manipulation and control, especially for low-volume biofluids such as sweat and interstitial fluid.[66–70] These strategies collectively improve sampling stability, reduce evaporation and contamination, and enable continuous or programmable sample delivery to downstream sensing modules. In fabricating microfluidic devices, the selection of flexible substrates is crucial.[71] Materials such as PDMS,[29,64] textiles,[72,73] paper-based substrates,[74,75] and hydrogels[76,77] provide excellent biocompatibility, flexibility, and stability to ensure device reliability and user comfort. These features support reliable long-term wear, reduce motion-induced artifacts, and help maintain consistent microfluidic behavior during on-body operation. Furthermore, advanced manufacturing techniques, such as photolithography,[68,78] 3D printing,[79,80] screen printing,[69,81] inkjet printing,[29,82] laser cutting,[81] etching,[64,83] evaporation,[77,84] two-photon polymerization,[85,86] and sputtering,[87–89] enable high-precision, scalable, and cost-effective production.[79,81,82] Together, these fabrication strategies support the development of microfluidic systems that are not only flexible and lightweight but also multifunctional, chemically robust, and compatible with large-scale production.

Currently, microfluidics-based flexible biosensors are evolving from single-function detection to intelligent, multifunctional systems.[90–92] As part of this transition, the integration of artificial intelligence for data analysis and cloud-enabled remote healthcare is emerging as a major trend.[35,93] Meanwhile, several wearable sensing platforms have entered the commercialization stage, indicating the growing demand and feasibility of real-world applications. Due to their significant advantages in non-invasive sampling, real-time monitoring, and user-friendly interfaces, wearable biosensors have also attracted extensive research interest from academia.

Numerous reviews have summarized recent advances in wearable sensor technologies, highlighting their sensing principles, target biomarkers, and potential applications.[2,3,94] For instance, Yu Cao *et al.* reviewed comprehensively wearable electrochemical sensors for non-invasive *in vitro* diagnosis, emphasizing advancements in fluid sampling, sensing mechanism, and materials for wearable microfluidic fabrication.[95] Wei Gao *et al.* reviewed recently developed photonic wearable biosensors and focused on how these sensors leverage the unique properties of light to achieve high-performance, non-invasive, real-time monitoring.[96] They pointed that targeting some other clinically valuable biomarkers is of great significance, which places high requirement on the sensitivity of devices. Tamoghna Saha *et al.* focused on harvesting and manipulating sweat and ISF for continuous and long-term sensing strategies using wearable patches.[65] They focused on sampling, extracting, transporting, and managing of microfluidics and excellently highlighted the future challenges that need to be resolved. Similarly, Navid Kashaninejad and Nam-Trung Nguyen reviewed recent on-skin wearable devices for biofluid monitoring.[97] They focused on how the highly stretchable and flexible microfluidic systems can be utilized to provide solutions for on-skin biofluid handling. They also presented in detail the future directions of wearable biosensors, including using droplet-based microfluidics, superhydrophobic surfaces and topological liquid diodes. Despite these comprehensive and excellent reviews, there remains a need to systematically address sensing strategies of microfluidics-integrated wearable biosensors tailored for specific biomarkers. We hope that the insights presented here will guide and inspire future research in wearable biosensing. For other healthcare-related analytes that are primarily addressed through chemical sensing approaches, such as wearable sensors for ion detection and pH monitoring, several comprehensive reviews have recently provided in-depth discussions and perspectives.[98–102]

Therefore, to maintain a clear focus and avoid redundancy, these chemical sensing strategies are not covered in the present review.

This review summarizes recent progress in wearable biosensing technologies by organizing detection strategies into three major analyte categories: metabolites, proteins, and nucleic acids. For each category, we highlight representative sensing mechanisms, sampling and integration approaches, and device designs relevant to on-body operation. The metabolite sections introduce microneedle-based extraction, non-invasive electrical and optical sensing, and emerging multimodal systems. The protein section compares label-free and labeled electrical and optical platforms, while the nucleic acid section discusses sampling strategies, amplification methods, and amplification-free approaches with potential for wearable use. By outlining these technologies within a clear framework, we aim to provide a concise reference that supports the development of practical, real-time, and personalized wearable health monitoring systems.

Overall principles for wearable biosensors

Wearable biosensors have advanced rapidly and now show exceptional promise in healthcare. A key enabler of this progress is the integration of microfluidics, which streamlines biofluid sampling, transport, and analysis within miniaturized, flexible platforms. Fig. 1 summarizes the major technologies underpinning these devices. Fig. 1A highlights the broad range of biofluids—tears, exhaled breath, saliva, sweat, blood, exudate wound, and interstitial fluid (ISF)—that

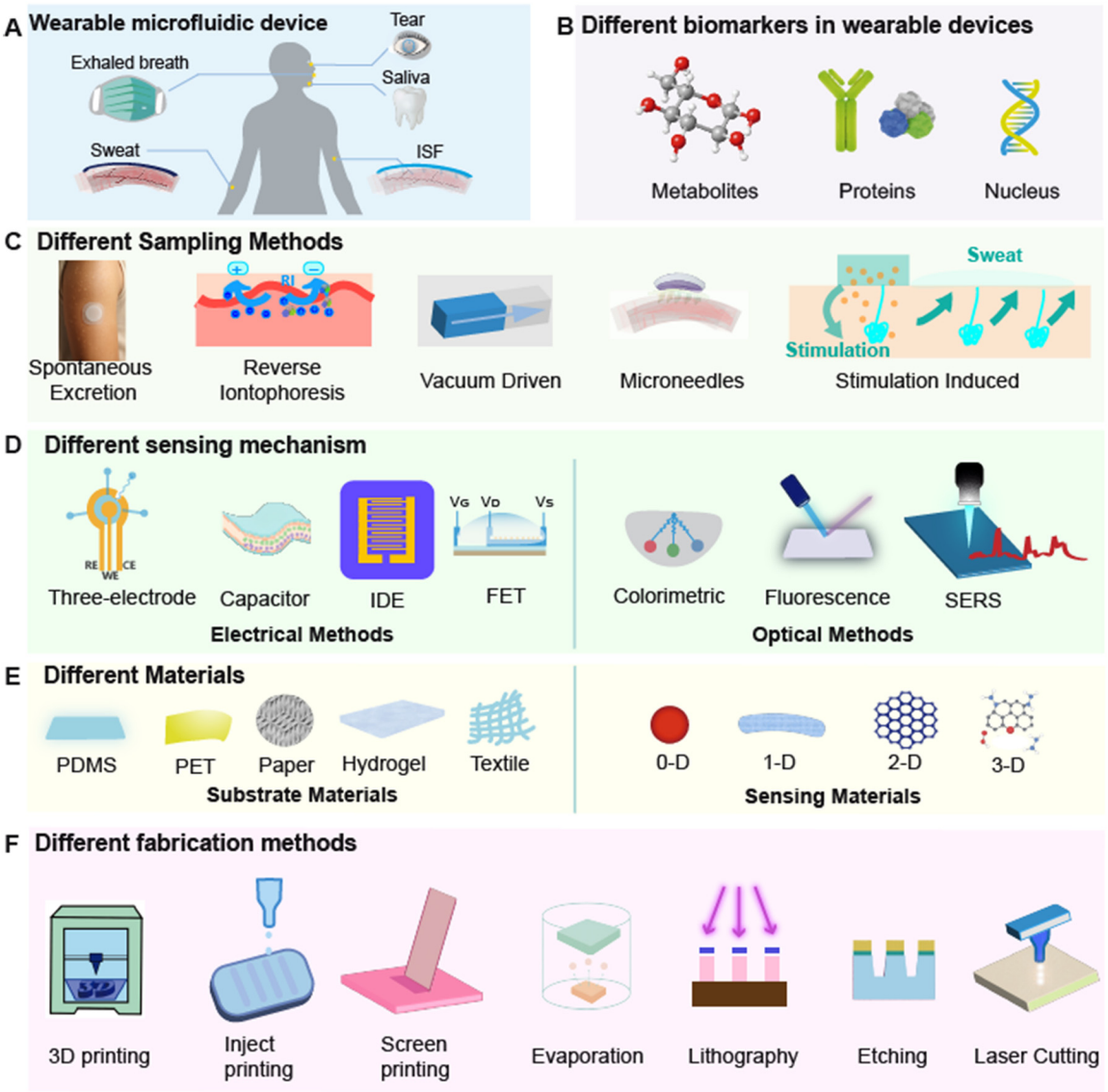

Fig. 1 Wearable microfluidic biosensors for health monitoring. Wearable biosensors collect (A) various biofluids, (B) detect key biomarkers, (C) using different sampling methods, and employ (D) diverse sensing mechanisms. They are built from (E) flexible substrates and functional materials, and fabricated *via* (F) multiple microfabrication methods.

can be collected through minimally or non-invasive means. Smart contact lenses and eye patches enable real-time monitoring of tear biomarkers; oral patches support *in situ* sensing and drug delivery *via* saliva; electronic masks capture breath condensate; and microneedle arrays or flexible electrode patches facilitate ISF and sweat analysis.

The principal biomarker classes accessible to wearable biosensors—metabolites, proteins, and nucleic acids—are shown in Fig. 1B. All three classes are pivotal for health surveillance and disease diagnosis. Metabolites, such as glucose, lactate, and uric acid (UA), respond rapidly to physiological changes, enabling real-time monitoring of metabolic disorders; their detection is typically based on enzymatic reactions. Proteins (*e.g.*, CRP, IL-6, TNF-α) offer high clinical specificity and diagnostic accuracy, with detection usually relying on antigen–antibody interactions. Nucleic acids, including DNA and RNA, can indicate early stages of disease, and their detection is generally based on DNA hybridization or polymerase chain reaction (PCR).

In wearable biosensors, various sampling methods are used, including spontaneous excretion, reverse iontophoresis, vacuum-driven extraction, microneedles, and stimulation-induced collection (Fig. 1C). Spontaneous excretion collects biofluids (such as sweat, tears, or saliva) directly from the skin, eyes, or mouth. Reverse iontophoresis uses an electric field to extract ions across membranes. Vacuum-driven extraction relies on suction to obtain samples. Microneedles penetrate the skin to access deeper biofluids. Stimulation-induced methods apply external triggers (like heat or electricity) to prompt sweat secretion for collection. Each approach has unique advantages, allowing flexible adaptation for different monitoring and analysis needs.

Fig. 1D provides an overview of the sensing mechanisms. To extract meaningful information from these biomarkers, wearable biosensors employ a variety of signal transduction strategies. Electrical approaches include electrochemical systems, in which analyte recognition or catalytic reactions at the working electrode induce changes in current or potential, capacitors, which can lead to changes in conductivity and permittivity upon recognition, and field-effect transistors (FETs), which transduce binding events or catalytic activity into shifts in the transfer curve. Optical methods encompass colorimetry, fluorescence, Raman spectroscopy (SERS), and other luminescent readouts, offering intuitive and rapid diagnostics well suited for point-of-care screening. Some of these methods usually demonstrate higher sensitivity and specificity, making them ideal for detecting low-abundance biomarker detection.

Material selection is equally critical (Fig. 1E). Common flexible substrates—PDMS, PET, paper, hydrogels, and textiles—offer biocompatibility, mechanical compliance, breathability, and chemical stability. For sensing layers, nanomaterials across dimensionalities are widely employed: 0-D materials such as quantum dots (QDs) and gold nanoparticles (AuNPs), 1-D materials such as nanowires and nanotubes, 2-D materials such as graphene or other nanosheets, and 3-D materials like hydrogels or metal–organic frameworks.

Finally, fabrication technology underpins device performance (Fig. 1F). Additive methods—3D printing, inkjet printing, screen printing, and physical vapor deposition—and subtractive methods—UV lithography, soft lithography, wet etching, and dry etching—jointly address the demands of miniaturization, mechanical flexibility, scalable production, and high analytical precision. Together, these advances are propelling wearable biosensors toward cost-effective, sensitive, and comfortable solutions for continuous health monitoring.

Wearable biosensors for metabolites

Wearable biosensors play a critical role in the detection of metabolic biomarkers including glucose, uric acid, and lactate in body fluids. One of the most important and significant metabolites is glucose due to its application in diagnosing diabetes. Accurate and timely monitoring of glucose levels is critically important for effective diagnosis, treatment, and management of diabetes. Although traditional glucose measurement methods, such as venous or finger-prick blood sampling, have been widely used clinically, they cannot effectively capture the dynamic fluctuations of glucose throughout the day due to influences from diet, physical activity, and other factors. Moreover, these invasive methods often cause discomfort and trauma to the patient. Therefore, minimally invasive, or non-invasive continuous glucose monitoring (CGM) has become highly desirable. CGM systems generally detect glucose fluctuations within ISF beneath the skin, where glucose levels closely correlate with blood glucose concentrations. Recent studies have validated the accuracy and efficacy of CGM technologies, demonstrating their capability to perform dynamic, real-time glucose monitoring with minimal discomfort.[103–105]

In addition to glucose, key metabolites such as uric acid (UA) and lactate are also present and hold significant diagnostic value. UA is the final product of human purine metabolism, and abnormal concentrations of uric acid are closely associated with various diseases.[106] It can be utilized in critical clinical research areas such as the early diagnosis of gout, risk assessment of chronic kidney disease (CKD), and prediction of cardiovascular disease risks (CVD).[107] Lactate, a byproduct of anaerobic metabolism, reflects physical exertion and muscle fatigue when detected in sweat, and its accumulation is a recognized biomarker for critical conditions such as shock, sepsis, and heart failure. Therefore, wearable lactate biosensors hold great promise for continuous monitoring in clinical settings like intensive care units (ICUs).

This section summarizes recent advances in wearable biosensors for metabolite monitoring and organizes current technologies according to their sensing approaches. We first discuss non-invasive electrical and optical sensing platforms, which enable on-skin detection of metabolites without penetrating the tissue. We then introduce minimally invasive microneedle-based systems that access interstitial fluid for continuous biochemical monitoring. Finally, we outline future development directions, including closed-loop

diabetes management and multimodal sensing, which represent promising pathways toward more autonomous and clinically meaningful wearable health technologies.

Non-invasive electrical methods for metabolite monitoring

Wearable biosensors based on sweat, saliva, or tears represent promising non-invasive methods for glucose monitoring.[108,109] These biosensors eliminate the need for blood sampling, enabling patients to comfortably wear them for long-term, continuous tracking of glucose levels. Among these, sweat-based glucose biosensors have been extensively studied.[110] Recent advancements in electrode materials, non-enzymatic systems, and microfluidic architectures have significantly enhanced the performance, sensitivity, and integration capabilities of wearable biosensors for metabolite detection.[111–113] This section summarizes key developments in material innovation and device engineering strategies that

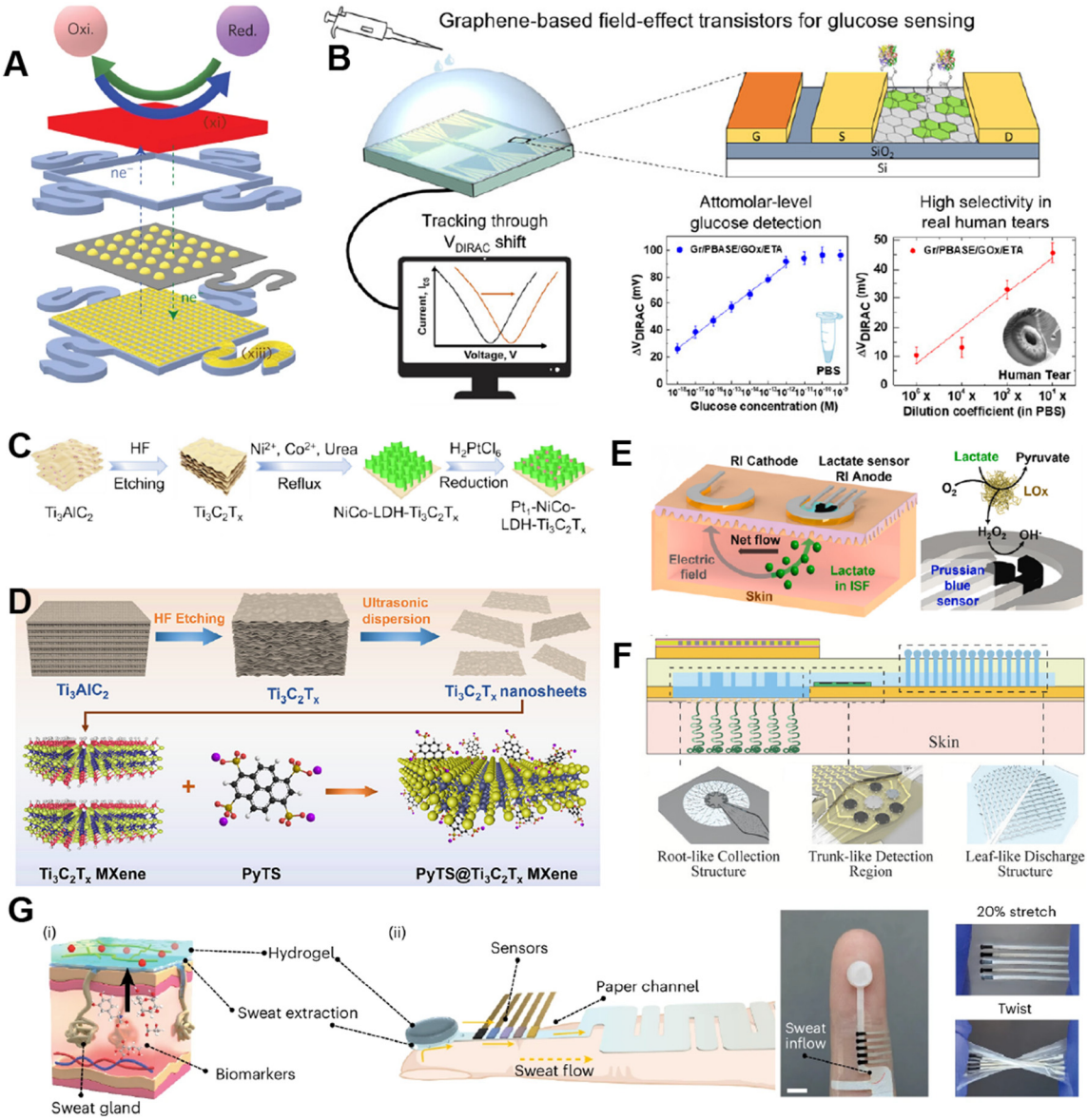

Fig. 2 Non-invasive electrochemical methods for metabolite monitoring. (A) Gold-doped graphene/gold mesh composite structure for high sensitivity metabolite monitoring. Reproduced from ref. 147 with permission from Springer Nature. (B) Electrolyte-gated graphene field-effect transistor (EG-GFET) for high performance glucose sensing. Reproduced from ref. 127 with permission from John Wiley and Sons. (C) Anchoring of single-atom Pt on a NiCo-LDH/$Ti_3C_2T_x$ heterostructure to enhance detection performance. Reproduced from ref. 41 with permission from American Chemical Society. (D) Anchoring PyTS onto the surface of $Ti_3C_2T_x$ to enhance detection performance. Reproduced from ref. 121 with permission from American Chemical Society. (E) 3D-structured microfluidic reaction chamber to increase the effective electrode surface area and reduce inter-electrode spacing, thereby enhancing signal strength. Reproduced from ref. 122 with permission from Elsevier. (F) A tree-branch-inspired microfluidic structure to expand the collection area for continuous tracking. Reproduced from ref. 125 with permission from John Wiley and Sons. (G) A fingertip-wearable micro-energy system utilizing hydrogel-based osmotic pumps for passive sweat extraction. Reproduced from ref. 126 with permission from Springer Nature.

support reliable and continuous metabolite analysis in wearable biosensors.

To achieve robust, long-term glucose monitoring in tears, Su-Kyoung Kim *et al.* proposed a nanoporous hydrogel embedded with bimetallic nanocatalysts designed for smart contact lenses.[114] Specifically, gold–platinum nanoparticles (Au@Pt) modified hyaluronic acid (HA-SH) to form HA-Au@Pt bimetallic nanocatalysts (HA-Au@Pt BiNCs), significantly enhancing catalytic activity and stability. Animal experiments showed a strong correlation between tear glucose and blood glucose concentrations (Pearson's coefficient ρ = 0.82), highlighting potential clinical significance. Additionally, Dingxi Lu *et al.* introduced an electrochemical mouthguard sensor utilizing platinum-based metallic hydrogels (PMH) for saliva glucose detection.[115] This sensor exhibited high sensitivity, excellent anti-interference capability, and strong clinical agreement, providing a practical solution for non-invasive diabetes monitoring.

Recent years have witnessed remarkable progress in constructing high-performance biosensors through advanced materials. Hyunjae Lee *et al.* innovatively employed a gold-doped graphene/gold mesh composite structure to significantly enhance the electrochemical activity of graphene electrodes, successfully developing a sweat-based wearable patch for diabetes monitoring (Fig. 2A).[116] This breakthrough marked the first application of graphene materials in diabetes monitoring and drug delivery. Another notable example is the electrolyte-gated graphene field-effect transistor (EG-GFET) proposed by Vicente Lopes: this device leverages direct interaction between the electrolyte and graphene channel to form a high-capacitance electric double layer (EDL), effectively amplifying local charge variation signals (Fig. 2B).[117] Meanwhile, GOx immobilized on the graphene surface catalyzes glucose oxidation, leading to H_2O_2 accumulation near graphene and inducing p-type doping (manifested as positive Dirac point voltage shift), enabling detection at ultralow concentrations (aM level). This study achieved the first glucose detection in diluted tears with a sensitivity of 100 aM, establishing a new paradigm for non-invasive monitoring. The research by Yu Zhang *et al.* pioneered the anchoring of single-atom platinum (Pt) on the NiCo-LDH/$Ti_3C_2T_x$ (MXene) heterostructure, constructing a unique "2D–2D" sandwich network architecture (Fig. 2C).[118] In this design, the introduction of NiCo-LDH not only effectively mitigates the aggregation issue of $Ti_3C_2T_x$ nanosheets but also significantly accelerates electron transfer through strong interfacial interactions, elevating the kinetics of glucose electrocatalytic oxidation to new heights. This sensor achieves a sub-micromolar detection limit, perfectly meeting the requirements for detecting low-concentration glucose (10–200 μM) in sweat, and provides a novel design paradigm for the development of other metabolite biosensors.

While enzymatic biosensors traditionally employ enzyme to catalyze the oxidation, limitations in enzyme stability and cost have driven the development of non-enzymatic alternatives.[107,119] Yong Zhang *et al.* introduced Pt/Fe dual-atomic catalysts into a flexible wearable electrode patch.[120] By leveraging the synergistic effects between Fe and Pt atoms, the system demonstrated enhanced catalytic efficiency, with a high sensitivity of 184.27 μA mM^{-1} cm^{-2}, strong anti-interference capacity, and a broad detection range from 6.25 to 1500 μM. Similarly, Fan Chen *et al.* designed a novel non-enzymatic material by anchoring 1,3,6,8-pyrenetetrasulfonic acid tetrasodium salt (PyTS) onto the surface of $Ti_3C_2T_x$ (MXene) *via* π–π conjugation, forming PyTS@$Ti_3C_2T_x$ (Fig. 2D).[121] The aromatic rings and sulfonate groups of PyTS provide abundant redox-active sites, significantly enhancing the electrocatalytic oxidation of UA. This material offers enzyme-free stability, lower cost, faster response, a wide linear range (5–100 μM), and an impressive detection limit of 0.48 μM. Ernesto De la Paz *et al.* developed a wearable lactate patch based on reverse iontophoresis, wherein a mild electric current applied to the skin surface induces electroosmotic flow to drive negatively charged lactate molecules toward the anode (Fig. 2E).[122] A PVA hydrogel substrate was used to significantly enhance extraction efficiency, enabling practical and efficient lactate sampling.

Microfluidic architectures play a central role in wearable biosensors by enabling controlled fluid transport, efficient analyte sampling, and stable reaction environments—greatly enhancing overall sensing performance.[33,123–128] Guodong Liu *et al.* developed a 3D-structured microfluidic reaction chamber that increases the effective electrode surface area and reduces inter-electrode spacing, thereby enhancing signal strength.[124] The design also isolates sweat from direct skin contact to minimize temperature and contamination interference, allowing for stable, long-term, non-invasive glucose monitoring. Inspired by plant transpiration, Jiaqi Niu *et al.* introduced a tree-branch-inspired microfluidic structure that expands the collection area by 10–100 times compared to conventional layouts (Fig. 2F).[125] This design enables spontaneous sweat flow without external pumps, relying solely on material hydrophilicity and channel geometry (*e.g.*, capillary force), achieving complete sweat refresh within one minute while maintaining stable flow rates—ideal for continuous tracking.

Paper-based microfluidic platforms, leveraging strong intrinsic capillary action, have emerged as simple yet powerful tools for passive sweat sampling and autonomous fluid routing in wearable glucose sensing.[129] Their internal channels promote both passive fluid sampling and autonomous flow without external power sources or pumps, reducing device invasiveness and system complexity. Shichao Ding *et al.* developed a fingertip-wearable micro-energy system utilizing hydrogel-based osmotic pumps for passive sweat extraction (Fig. 2G).[126] Laser-patterned Whatman filter paper with serpentine channels served as fluid conduits, prolonging sweat retention time and ensuring adequate biochemical reaction. Shanshan Zhang *et al.* pioneered the integration of an electrochemical sensor array, microfluidic module, and iontophoresis electrode onto a single paper substrate.[127] Using wax printing and origami techniques, they created a low-cost, scalable platform. Conductive electrodes

treated with PPAAM-doped PEDOT: PSS ink retained paper porosity while improving conductivity and electrochemical activity, resulting in a highly sensitive yet economical wearable glucose sensor.

In summary, non-invasive electrical sensing technologies have made substantial progress in improving the sensitivity, selectivity, and integration of wearable metabolite biosensors, particularly for glucose, uric acid, and lactate monitoring in sweat, saliva, and tears. Innovations in advanced nanomaterials, microfluidic architectures, and electrode design have enabled real-time, continuous, and enzyme-free detection with high precision and low detection limits. These advancements provide a solid foundation for the development of next-generation closed-loop diabetes management systems, where continuous glucose monitoring can be integrated with therapeutic feedback.

Non-invasive optical methods for metabolite monitoring

Microneedle-based glucose biosensors, while reducing the discomfort associated with traditional blood sampling, remain minimally invasive and can still cause minor skin damage.[130] Recently, significant research efforts have been directed toward developing truly non-invasive glucose monitoring approaches.[131,132] Using microfluidic sampling and enrichment in combination with optical sensing has become a major non-invasive detection strategy. Optical approaches typically rely on either naked-eye colorimetric or SERS methods.

Colorimetric assays offer a distinct advantage because their signals can be read directly by the naked eye, making them a focal point of extensive research.[133,134] Xuecui Mei *et al.* developed a wearable nanofiber microfluidic analysis system (NFMAS) consisting of three core layers: (i) a nanofiber microfluidic network (NFMN), (ii) an electrochemical sensor array, and (iii) a colorimetric sensor array.[135] This architecture enables spontaneous sweat capture, directional transport, and dual-mode (electrochemical and colorimetric) sensing, providing high stability, strong anti-interference capability, a broad dynamic range, and high sensitivity (Fig. 3A). Yunyun Wu *et al.* developed a flexible, skin-interfaced microfluidic sensor in which capillary forces within PDMS microchannels guide sweat flow, while integrated capillary burst valves (CBVs) prevent backflow, as indicated in Fig. 3B.[51] A paper substrate loaded with enzymes generates a color change that enables non-invasive, real-time monitoring of β-hydroxybutyrate (BHB) in sweat. The device is low-cost, user-friendly, flexible, biocompatible, and simple to operate. Navya Mishra *et al.* achieved comparable results: by integrating a finger-actuated pump–valve with a microfluidic network, they overcame the passive nature of conventional sweat sensors.[40] The platform supports dual-mode readout—colorimetric signals captured by a smartphone camera and electrochemical measurements—enabling on-demand, time-resolved, multi-analyte sweat analysis (Fig. 3C).

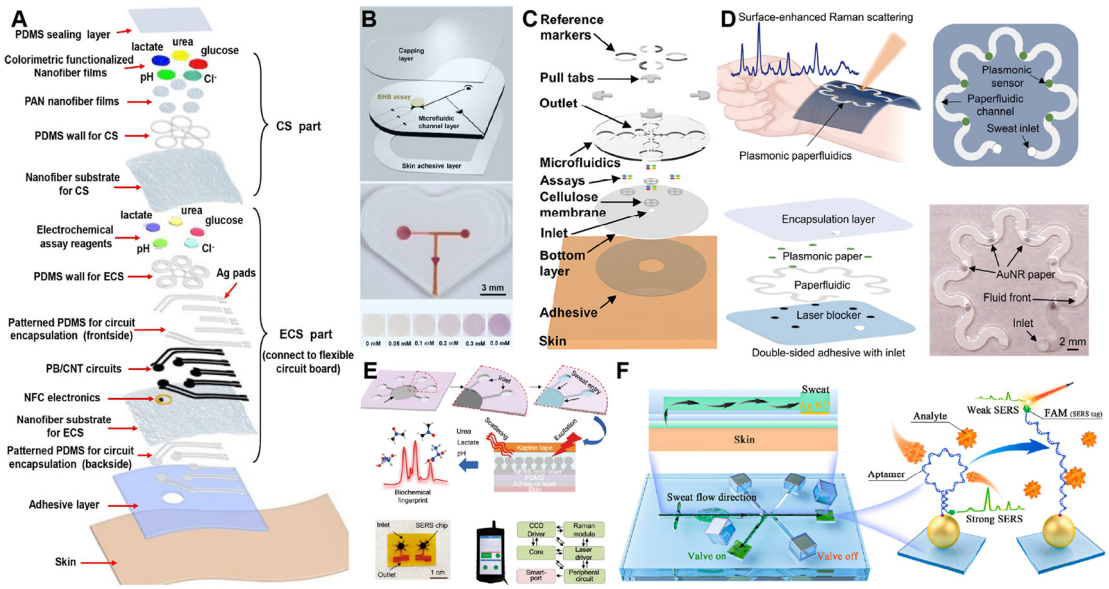

Fig. 3 Non-invasive optical strategies for metabolite monitoring. (A) Wearable NFMAS for spontaneous sweat capturing, directional transporting, and dual-mode (electrochemical and colorimetric) sensing. Reproduced from ref. 135 with permission from Elsevier. (B) A flexible, skin-interfaced microfluidic sensor integrated with PDMS microchannels and CBVs for BHB detection. Reproduced from ref. 51 with permission from The Royal Society of Chemistry. (C) A finger-actuated pump–valve combined with a microfluidic network device for dual-mode (electrochemical and colorimetric) sensing. Reproduced from ref. 40 with permission from American Chemical Society. (D) Label-free surface-enhanced Raman scattering (SERS) sensor based on plasmonic paper for sweat metabolite detection. Reproduced from ref. 140 with permission from American Association for the Advancement of Science. (E) A lightweight and user-friendly system consisting of a multi-channel sweat collection structure combined with an ultrathin silver nano-mushroom array for real-time molecular fingerprint analysis of sweat. Reproduced with permission from ref. 141 under a Creative Commons CC BY license. (F) A SERS-based wearable biosensor for continuous metabolite monitoring while minimizing interference from other sweat constituents. Reproduced from ref. 142 with permission from Elsevier.

Spectroscopy-based biosensors, especially SERS based devices, have drawn substantial attention due to their excellent comfort, non-invasiveness, and user-friendly characteristics.[136–139] Umesha Mogera *et al.* developed a high-performance wearable sweat analysis platform utilizing label-free surface-enhanced Raman spectroscopy (SERS), as shown in Fig. 3D.[140] By employing gold nanorods (AuNRs) to amplify the Raman signal, their device successfully captured the chemical fingerprint of UA, specifically at the characteristic peak of 642 cm^{-1}. This enzyme-free system offers exceptional sensitivity, enabling UA detection at as low as 1 μM. Similarly, Xuecheng He *et al.* developed a multi-channel sweat collection structure to improve sampling volume.[141] A rigid yet ultrathin (100 μm) silver nanomushroom array was used as a surface-enhanced SERS substrate, coupled with laser excitation, CCD detection, and wireless transmission modules (Fig. 3E). This lightweight and user-friendly system supports real-time molecular fingerprint analysis of sweat, offering a powerful tool for non-invasive molecular-level monitoring in personalized medicine and athletic health applications. To enable continuous metabolite monitoring while minimizing interference from other sweat constituents, Kuo Yang *et al.* developed a SERS-based wearable biosensor.[142] The device incorporates PDMS microchannels and a manual valve to permit multiple on-demand sampling events, while a self-assembled monolayer of silver nanospheres on the substrate boosts SERS sensitivity, allowing UA to be quantified over a 1–1000 μM concentration range (Fig. 3F). Likewise, Yang Li *et al.* designed a flexible, wearable plasmonic paper-based microfluidic (FWPPM) sensor that integrates SERS into a compact five-layer architecture, enabling real-time, non-invasive monitoring of uric acid in sweat.[39]

Minimally invasive microneedle biosensing for metabolite monitoring

Microneedle-based biosensors have emerged as an important class of wearable devices for minimally invasive metabolite monitoring. Depending on their structural design and sensing modality, microneedles consist of hollow microneedles for ISF extraction, solid microneedles with surface-functionalized coatings, or 3D-printed microneedles that integrate conductive or enzyme-loaded layers. These microneedles penetrate the skin's stratum corneum without reaching blood vessels or nerves, enabling access to ISF while avoiding trauma. To facilitate the widespread and reliable application of microneedle biosensors in metabolic monitoring, researchers have made substantial efforts in improving long-term stability, enhancing detection accuracy, promoting integrated designs, and optimizing wearer comfort.

Sampling strategies used in microneedle systems can be broadly classified into active and passive methods. To achieve high-throughput ISF collection, both active pumping mechanisms (such as vacuum actuation,[33] electroosmotic flow,[143] and reverse iontophoresis[144]) and passive enhancement strategies (*e.g.*, capillary action[145,146]) have been employed. These approaches aim to improve ISF extraction speed, consistency, and sampling volume—key requirements for reliable metabolite sensing. For instance, Taher Abbasiasl *et al.* proposed a vacuum-driven microneedle-based system that integrates a hollow microneedle with a finger-press-activated vacuum chamber, as shown in Fig. 4A.[33] Leveraging the self-recovery properties of PDMS, this system requires no external power source and was the first to demonstrate *in vivo* ISF sampling and electrochemical analysis of glucose and pH, offering a promising solution for continuous health monitoring. Similarly, Yanxiang Cheng *et al.* combined mechanical microneedle penetration with reverse iontophoresis, enabling glucose transport through uniform microchannels to sensing electrodes. The integration of microchannel access (MA) and reverse iontophoresis (RI) significantly enhanced ISF extraction efficiency.[123]

Beyond facilitating ISF extraction, the penetration characteristics of microneedles play a crucial role in determining how effectively microfluidic channels receive and route biofluids, thereby shaping the stability of the overall sensing process. To optimize penetration efficiency and provide practical guidance, Yong Yang *et al.* developed a microneedle penetration model.[147] Additionally, to improve sensor integration, they innovatively utilized PCB microvias and acupuncture needle assembly techniques, enabling each microneedle in the array to function as an independent electrode for multi-region, multi-parameter detection. In healthy volunteer trials, the system demonstrated strong agreement with commercial glucometer readings.

Material innovation is another important strategy for improving electrochemical performance in microneedle sensors. Novel sensing materials were widely applied, including platinum,[148] gold,[149] graphene,[150] carbon nanotubes[151,152] and polymer-based materials,[153–155] which are increasingly becoming key components due to their excellent conductivity, low cost, and superior stability.[156,157] The team led by Samar H. Tawakey innovatively developed a poly(methyl methacrylate) (PMMA)-based microneedle array sensor (Fig. 4B).[158] By electrodepositing a composite functional layer of nanostructured polyaniline (NSPANI) and gold nanoparticles (AuNPs), they achieved remarkable improvements in sensor performance. In this design, the three-dimensional nanostructure of NSPANI not only provides a larger specific surface area to enhance electron transfer efficiency but also, through synergistic effects with AuNPs, significantly boosts catalytic activity and surface binding site density, thereby optimizing the immobilization of glucose oxidase (GOx). Particularly noteworthy is the first successful application of the NSPANI-SDS/AuNPs composite mediator, which effectively addresses the longstanding industry challenge of balancing sensitivity and stability in traditional biosensors.

Achieving long-term (14 day) continuous glucose monitoring while improving wearer comfort is also of great significance. Jian Yang *et al.* developed a smartphone-controlled microneedle-based CGM system.[159] This system utilizes a flexible double-sided electrode strip integrating a working electrode (WE), reference electrode (RE), and counter electrode (CE), as shown in

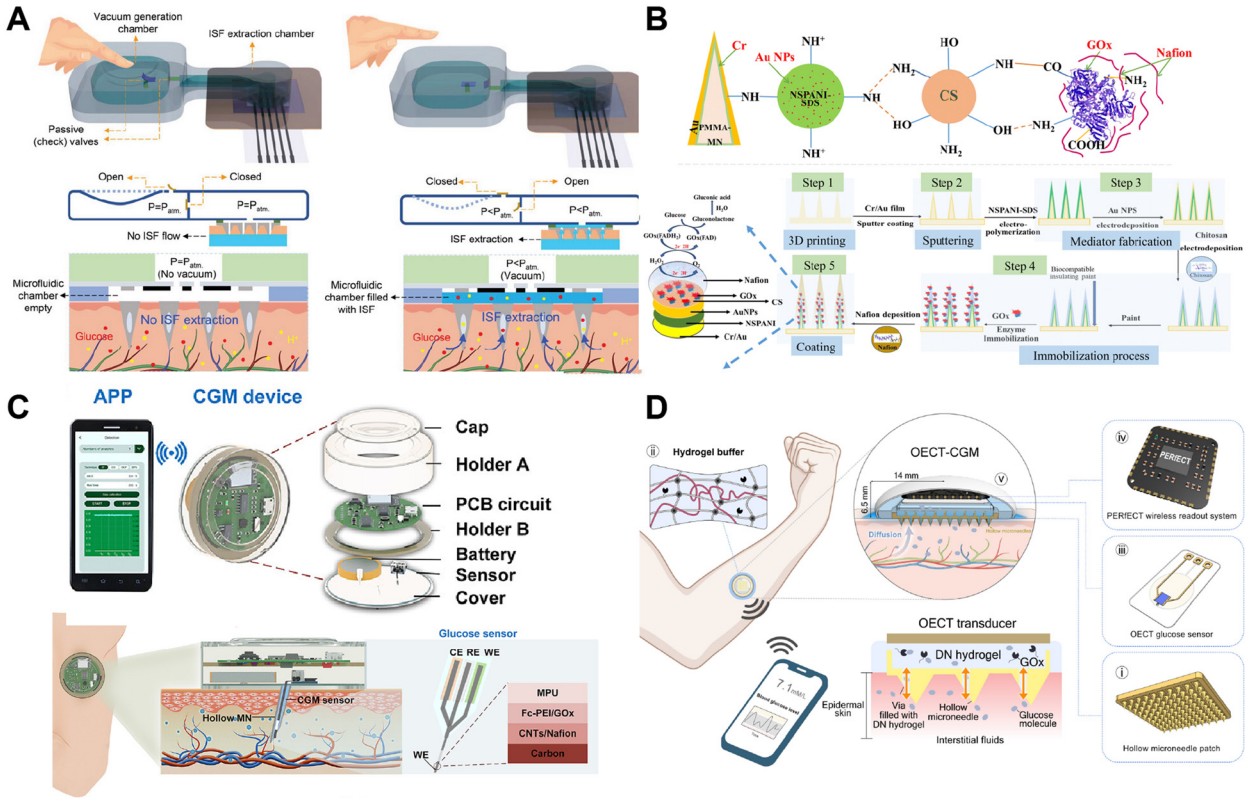

Fig. 4 Microneedle-based biosensors for metabolite monitoring. (A) Vacuum-assisted microneedle system integrating a hollow microneedle array with a fingertip-activated vacuum chamber to drive interstitial fluid (ISF) extraction. Reproduced from ref. 33 with permission from John Wiley and Sons. (B) PMMA-based microneedle array sensor modified with conductive nanocomposites to enhance sensitivity. Reproduced from ref. 158 with permission from The Royal Society of Chemistry. (C) Smartphone-integrated continuous glucose monitoring (CGM) platform featuring a hollow microneedle sensor and a 14 day wearable module. Reproduced from ref. 159 with permission from American Chemical Society. (D) Fully integrated OECT-CGM system. i: Hollow microneedle patch for sampling. ii: Hydrogel buffer for glucose transport. iii: OECT glucose sensor for detection. iv: Wireless readout system for data transmission. v: Schematic of the complete implantable patch showing cross-section and scale. Reproduced with permission from ref. 104 under a Creative Commons CC BY license.

Fig. 4C. To enhance sensor stability, the team designed a sandwich-structured enzyme immobilization strategy: the inner layer consists of a carbon nanotube (CNTs)/Nafion conductive layer to establish an efficient electron transport network; the middle layer employs ferrocene derivatives (Fc-PEI) as an electron mediator, forming a "molecular wire" structure with glucose oxidase (GOx); and the outer layer is coated with a biocompatible porous polyurethane (MPU) protective membrane to minimize foreign body reactions and improve long-term stability. In healthy rat models, the system successfully achieved 14 day continuous glucose monitoring, with data strongly correlating ($R^2 > 0.99$) with commercial glucometers (Sinocare) and FDA-approved CGM devices (FreeStyle Libre). These results demonstrate that long-term microneedle-based CGM is feasible and well-tolerated for continuous wearable glucose monitoring.

Beyond material engineering, device-level innovations have also been explored to further enhance signal quality and long-term stability. Organic electrochemical transistors (OECTs), known for their high signal amplification, superior signal-to-noise ratio, and high gain, offer another promising strategy to enhance sensor stability and detection accuracy. Jing Bai *et al.* innovatively integrated OECTs (high gain), microneedles (minimally invasive), hydrogels (stable interface), and a personalized electronic reader for electrochemical transistors into a single wearable device (Fig. 4D), effectively addressing the pain, noise interference, and bulkiness of conventional CGM systems.[104]

The diversity of microneedle structures—including hollow, solid, and coated designs—also enables different sensing modes for various metabolites. Microneedle-based wearable biosensors represent a minimally invasive strategy for continuous metabolite monitoring, particularly for analytes such as glucose and lactate. This section outlines advances in microneedle fabrication and sampling mechanisms, including vacuum actuation and reverse iontophoresis, as well as their integration with sensing systems, such as electrochemical electrodes and organic electrochemical transistors (OECTs). Efforts have focused on enhancing sampling efficiency, improving material design, optimizing sensor architecture, and extending operational stability. Future research will need to address challenges such as ensuring long-term biocompatibility, minimizing skin irritation during extended wear, and improving the accuracy of detection under dynamic physiological conditions. In addition, integration with wireless data

transmission, energy autonomy, and closed-loop feedback systems remains a key direction for realizing fully autonomous wearable diagnostic platforms.

Future directions of wearable metabolite biosensors

Wearable metabolite biosensors are moving toward higher levels of integration and autonomous functionality. One important direction is the development of closed-loop metabolic management, where continuous sensing is combined with automated feedback control to enable intelligent regulation of glucose and other key metabolites. Another emerging trend is multimodal sensing, which integrates electrical, optical, and physical signals to improve measurement robustness, reduce calibration drift, and provide more comprehensive physiological insights. Together, these advances reflect the broader transition from single-parameter monitoring to adaptive, personalized, and clinically meaningful wearable systems.

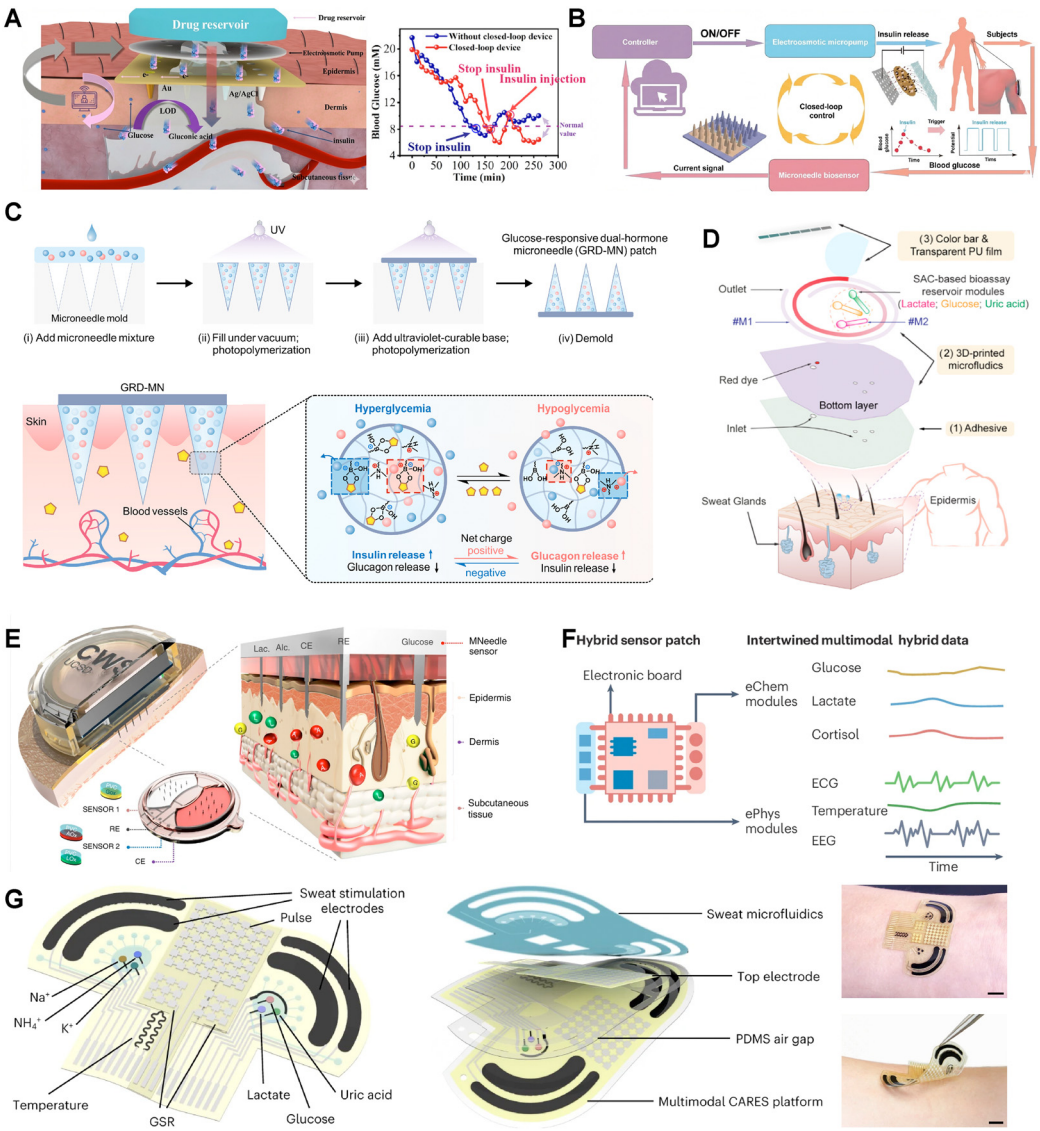

Fig. 5 Diabetes management strategies. (A) A closed-loop diabetes Minipatch for blood glucose stabilization and diabetes management. Reproduced from ref. 143 with permission from American Chemical Society. (B) Schematic of a closed-loop diabetes management device for alternative glucose sensing and insulin delivery. Reproduced from ref. 161 with permission under a Creative Commons CC BY license. (C) A glucose-responsive dual-hormone microneedle patch (GRD-MN) enabling closed-loop blood glucose control. Reproduced from ref. 168 with permission from American Association for the Advancement of Science. (D) A flexible 3D-printed microfluidic device fabricated *via* direct ink writing (DIW) for monitoring glucose, lactate, and uric acid. Reproduced from ref. 163 with permission from American Chemical Society. (E) A wearable sensor array that integrates disposable microneedle arrays with a reusable low-power electronic module capable of wireless transmission for monitoring glucose, lactate, and alcohol. Reproduced from ref. 92 with permission from Springer Nature. (F) Multimodal detection strategies by Kuldeep Mahato for better diabetes management. Reproduced from ref. 169 with permission from Springer Nature. (G) Consolidated artificial-intelligence-reinforced electronic skin designed for stress response monitoring *via* integrated physiological and biochemical sensing including ions, lactate, glucose, and uric acid. Reproduced from ref. 93 with permission from Springer Nature.

Closed-loop diabetes management. Benefiting from the advances in wearable sensing technology, closed-loop diabetes management systems have been further developed and are expected to become a benchmark solution for intelligent, non-invasive diabetes care. These systems typically integrate continuous glucose monitoring (CGM), real-time data processing, and on-demand insulin delivery into a single wearable platform, enabling automated feedback control of blood glucose levels. By combining microneedle-based ISF extraction, electrochemical sensing, and microfluidic drug release modules, such platforms aim to mimic the physiological regulatory functions of the pancreas, offering personalized and dynamic glucose regulation.

Hyunjae Lee *et al.* firstly used graphene doped with gold to construct a wearable patch for sweat-based diabetes monitoring and feedback therapy.[116] After that, a fully-electrically controlled closed-loop diabetes management system has been studied. Xiaojin Luo *et al.* developed an innovative flexible closed-loop diabetes management patch, which integrates hollow biodegradable microneedle arrays, electrochemical sensors, and an electroosmotic pump to achieve real-time monitoring of interstitial fluid (ISF) glucose and on-demand insulin delivery in a closed-loop system (Fig. 5A).[143] Yiqun Liu *et al.* studied a painless, closed-loop, and miniaturized solution for diabetes management through the innovative integration of hollow microneedle dual-function design and modified electroosmotic pumps, demonstrating enhanced stability and anti-interference capability (Fig. 5B).[161] Furthermore, Changwei Yang *et al.* developed a glucose-responsive dual-hormone microneedle patch (GRD-MN) that integrates insulin and a glucagon-like analog (GCA) to mimic the pancreatic hormonal regulation mechanism, enabling closed-loop blood glucose control (Fig. 5C).[168]

Closed-loop systems are showing significant potential in diabetes management. However, the realization of fully autonomous, clinically reliable closed-loop systems still faces several challenges, including ensuring long-term biosensor stability, minimizing the time lag between changes in biomarker concentration and the sensing response, and achieving precise insulin dosing under variable physiological conditions.

Multimodal and multiplexed metabolite detection. Simultaneous monitoring of multiple metabolites, also known as multiplexed detection, enables a more comprehensive assessment of an individual's metabolic status and overall physiological health. By tracking multiple biomarkers such as glucose, lactate, uric acid, and others within a single platform, multiplexed systems provide a more holistic view of metabolic dynamics and interrelated physiological processes. This approach allows for the early identification of complex conditions, supports more accurate diagnosis, and facilitates personalized health management. Furthermore, the combination of microfluidics, multi-channel sensing arrays, and flexible substrates opens new opportunities for multimodal analysis of multiple metabolites, offering a more comprehensive and personalized approach to metabolic health monitoring.

Chuchu Chen introduced a flexible 3D-printed microfluidic health monitor fabricated *via* direct ink writing (DIW), which enables one-step formation of self-supporting microchannels without the need for sacrificial material removal (Fig. 5D).[163] By replacing traditional enzymes with Fe–N–C single-atom catalysts (SACs), the device dramatically enhanced the sensitivity and stability of colorimetric detection for glucose, lactate, and uric acid, improving the assay's sensitivity by nearly two orders of magnitude. In another work, Farshad Tehrani *et al.* reported a novel wearable sensor array that integrates disposable microneedle arrays (for painless ISF sampling) with a reusable low-power electronic module capable of wireless transmission (Fig. 5E).[92] This platform supports both single-analyte (*e.g.*, glucose, lactate, alcohol) and dual-analyte (*e.g.*, glucose–lactate, glucose–alcohol) monitoring. The use of spatially separated microelectrodes effectively prevents signal interference, providing a robust tool for personalized diagnostics.

In a recent review by Kuldeep Mahato, the author emphasized that patients with diabetes require simultaneous monitoring of blood glucose, blood pressure, and electrocardiogram (ECG) signals to achieve more comprehensive disease management, which is multimodal biosensing (Fig. 5F).[169] Furthermore, the author proposed a paradigm shift from static biomarker monitoring to dynamic tracking of pathological processes. For instance, the concurrent elevation of lactate and inflammatory cytokines such as IL-6 may serves as an indicator of muscle injury severity. Integrating multiple metabolic indicators into a single wearable platform facilitates the development of multiparametric, real-time personalized health monitoring systems, thus enabling a shift from passive treatment to proactive prevention and promoting the advancement of smart healthcare and remote diagnostics. In recent years, research on multimodal sensing in wearable devices has grown increasingly extensive and in-depth.[4,169,170]

As a typical application of multimodal sensing scheme, an advanced electronic skin system termed CARES (consolidated artificial-intelligence-reinforced electronic skin) was introduced by Changhao Xu, which is designed for stress response monitoring *via* integrated physiological and biochemical sensing (Fig. 5G).[93] In sensor design, a Prussian blue/NiHCF composite was used to stabilize enzymatic activity and protect against pH-induced degradation from sweat. A polystyrene–ethylene–butylene–styrene (SEBS) layer was incorporated to enhance the hydrophobicity of the PVC substrate, minimizing ion carrier leakage. Iontophoresis-driven sweat stimulation was achieved using carbachol, ensuring sweat secretion under resting conditions and avoiding exercise-induced interference. After 24 hour continuous monitoring of daily activities—including eating, exercise, and sleep—the system successfully captured dynamic biomarker variations (*e.g.*, postprandial rises in glucose and uric acid, and electrolyte fluctuations during physical activity). By integrating material innovation, AI, and

multimodal sensing, CARES overcomes limitations of traditional stress monitoring and offers a new paradigm for wearable technologies in psychological health applications.

To sum up, this section provides a systematic overview of wearable biosensors for metabolite detection, with a particular emphasis on their application in non-invasive and continuous monitoring. The main types of biofluids utilized, the corresponding sensing strategies, and the materials and fabrication techniques that support device performance are outlined. Minimally invasive microneedle-based biosensors, non-invasive optical methods, and biofluid-based detection systems have each demonstrated promising progress in enhancing comfort, accuracy, and long-term usability. Some representative works are summarized in Table 1. At the same time, innovations in sensing materials—such as nanostructured polymers, single-atom catalysts, and 2D heterostructures—have pushed sensitivity to unprecedented levels. Meanwhile, microfluidic engineering has enabled efficient fluid sampling and integration, supporting robust on-body analysis. However, the correlation mechanisms between biofluids and blood glucose, as well as anti-interference capabilities, still require further investigation. In the future, innovations in nanomaterials and system integration are expected to enhance sensor sensitivity,

Table 1 Comparative analysis of wearable biosensors for metabolite sensing

Biofluid	Biomarkers	Sensing mechanism	Material	Fabrication method	Ref
ISF	Glucose	FET	PI substrate, PEDOT: PSS, IPN hydrogel, GOx	Sputtering, inkjet printing, 3D printing,	104
ISF	Glucose	Electrochemical	PB, GOx	PDMS molding, PVD, laser cutting	143
ISF	Glucose	Electrochemical	PDMS, PET, PB, PANI	PDMS molding, screen printing	32
ISF	Glucose, lactate	Electrochemical	MeHA hydrogel	PDMS molding, UV crosslinking	103
ISF	Glucose	Electrochemical	PB, GOx	Laser cutting, 3D printing	147
ISF	Glucose	Electrochemical	PB, Gox, TPU	Soft lithography, sputtering, 3D printing	77, 160
ISF	Glucose	Electrochemical	Au-MCNT, MB, graphene, Gox,	Ink-printed, PVD,	161
ISF	Urea	Electrochemical	PABA, Au, Ag/AgCl, urease enzyme, Nafion	3D printing, soft lithography, sputtering, dip-coating	80
ISF/sweat	Glucose, lactate	Electrochemical	SEBS copolymer, hydrogels, graphene, PB, PVDF	Laser cutting, screen printing	4
Sweat	Glucose	Electrochemical	AuNPs/AMWCNTs, PEDOT:PSS, Ag/AgCl	Screen printing	162
Sweat	Urea	Fluorescence	PAM, Er/Tm@$NaYF_4$, *p*-DMAC	Hydrogel molding, 3D printing	133
Sweat	Glucose	Colorimetric	PVA hydrogel, HRP, Gox	Physical crosslinking	155
Sweat	BHB	Colorimetric	PDMS, paper,	3D printing, PDMS molding	51
Sweat	Glucose	Electrochemical	PET, Pt_1–NiCo-LDH/$Ti_3C_2T_x$	Screen printing	118
Sweat	Glucose, lactate, VC, L-dopa	Electrochemical	Paper, SEBS copolymer, PVA–PAM hydrogels	Laser cutting, screen printing	126
Sweat	Glucose, lactate, UA, ions, pulse, temperature	Electrochemical	PI substrate, PVC–SEBS, PDMS, Ag/carbon, AuNPs	Inkjet printing, laser cutting, etching	93
Sweat	Lactate, urea	SERS	Si nanopillar arrays, PDMS	Sputtering, RIE etching, soft lithography	141
Sweat	Glucose, lactate, UA	Colorimetric	Fe–N–C nanozyme	DIW	163
Sweat	UA	SERS	Cellulose paper, AuNRs, PDMS.	Spin coating	140
Sweat	Glucose	Colorimetric	PDMS, paper, AuNRs, GOx	Laser cutting	164
Sweat	Glucose	Electrochemical	CuO/$CaTiO_3$/Nafion composite, Au-sputtered PI film, Ag/AgCl/PVB	Sputtering	165
Sweat	Glucose, creatinine, UA	Electrochemical	Paper, PEDOT:PSS/AAM conductive ink, Ag/AgCl, wax, PB	Wax printing, 3D printing	127
Tear	Glucose	Optical	Hydrogel	Replica molding, drop-casting	109
Tear	Glucose	Electrochemical	PVA, HA-Au@Pt, silicone elastomer	Drop-casting	114
Tear	UA	Colorimetric	Fluorosilicone acrylate, HRP, PDMS	Laser ablation, 3D printing	166
Saliva	Glucose	Electrochemical	Pt, Ag/AgCl, PDMS, GOx	Sputtering, drop casting	108
Saliva	Glucose	Electrochemical	PMH/Nafion, Ag/AgCl	Screen printing	115
Sweat/saliva/urine	UA	Electrochemical	PET, 3D-NSCAs	Screen printing, laser cutting	167

DIW: direct ink writing, PB: Prussian blue, GOx: glucose oxidase, PVD: physical vapor deposition, MeHA: methacrylated hyaluronic acid, BHB: β-hydroxybutyrate, MB: methylene blue, MCNT: multiwall carbon nanotubes, SEBS: styrene–ethylene–butylene–styrene block copolymer. VC: vitamin C. L-dopa: levodopa. PI: polyimide. PVC: polyvinyl chloride. AuNPs: Au nanoparticles. SERS: surface-enhanced Raman spectroscopy. RIE: reactive ion etching. IPN: interpenetrating network. AuNRs: Au nanorods. AMWCNT: aminated multi-walled carbon nanotubes. PVA: polyvinyl alcohol. HA: hyaluronate. PMH: Pt metal hydrogel. 3D-NSCAs: 3D nitrogen-doped spherical carbon aerogels. PABA: polyaniline boronic acid. PAM: polyacrylamide. *p*-DMAC: *p*-dimethylaminocinnamaldehyde.

specificity, and user-friendliness, driving forward the development of personalized diabetes care.

Wearable biosensors for proteins

Proteins are one of the most essential and abundant types of biomacromolecules in the human body. Dynamic changes in their concentrations can serve as critical indicators for the onset and progression of various diseases. With advancements in wearable sensor technologies, it has become feasible to achieve automated, *in situ*, and continuous monitoring of protein levels in biofluids. However, wearable protein sensing remains in its early stages, primarily limited by challenges in effective sample collection and insufficient detection sensitivity. Current research efforts are mainly focused on skin-patch-based detection of C-reactive protein (CRP) and inflammatory cytokines, as well as tear-fluid-based protein sensing.[37] Studies have demonstrated that CRP is indeed present in the sweat of healthy individuals, and its concentration in sweat shows a high correlation with serum levels in both healthy and inflammatory populations, providing a theoretical foundation for sweat-based wearable protein detection.[171]

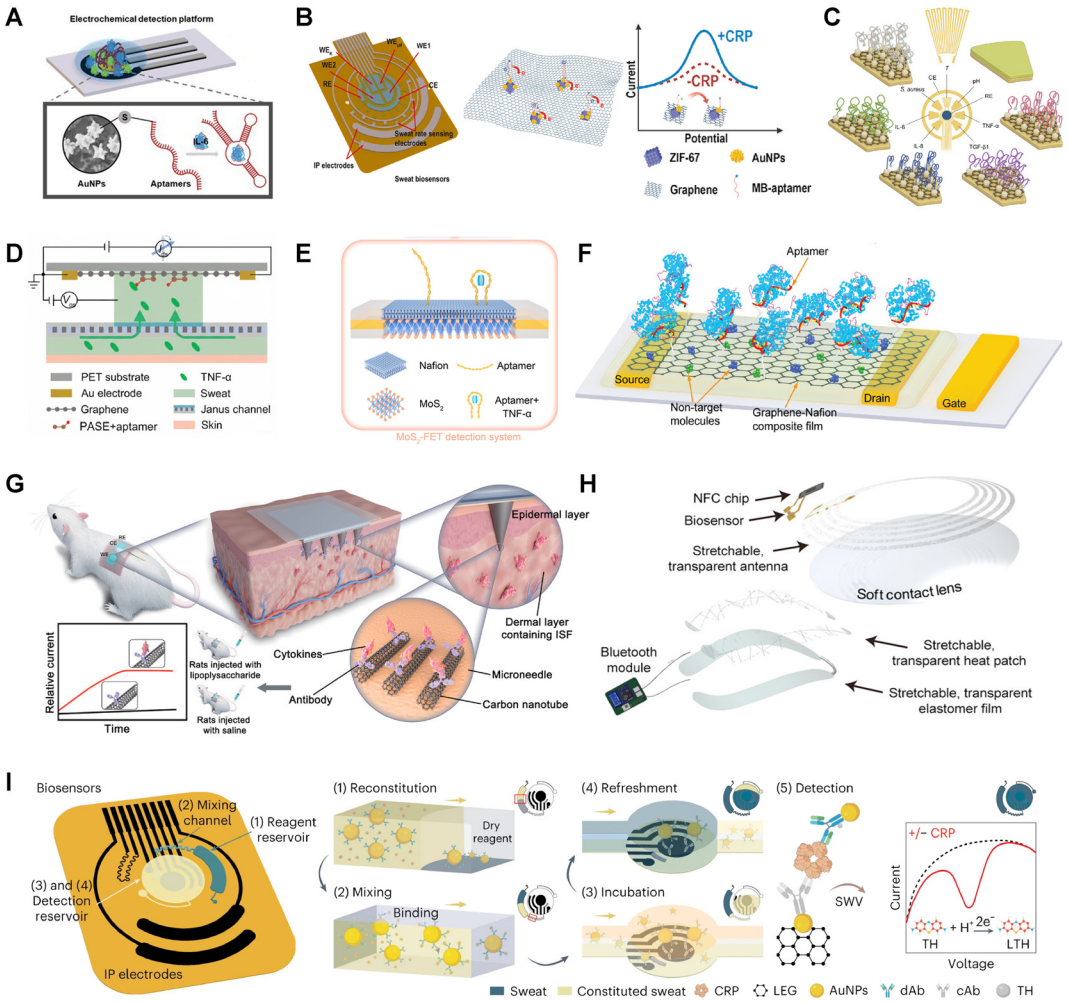

Fig. 6 Wearable biosensors for proteins in ISF and sweat. (A) The basic structure of a three-electrode system used for protein detection. Reproduced from ref. 37 with permission under a Creative Commons CC BY license. (B) ZIF-67@AuNPs nanocomposite with a high surface area and conductivity to enhance sensitivity in sweat CRP detection. Reproduced with permission. Reproduced from ref. 175 with permission from Elsevier. (C) A flexible integrated wound monitoring platform for multiplex detection of inflammatory biomarkers including TNF-α, IL-6, IL-8, and TGF-β1. Reproduced with permission. Reproduced from ref. 31 with permission under a Creative Commons CC BY license. (D) Flexible graphene FET biosensor integrated with a Janus membrane enables automatic sweat sampling and continuous, label-free detection of cytokines on skin. Reproduced from ref. 172 with permission from John Wiley and Sons. (E) Flexible MoS_2 FET platform for automatic sweat collection and real-time TNF-α monitoring. Reproduced from ref. 178 with permission from American Chemical Society. (F) A FET based protein wearable sensor on a flexible substrate. Reproduced from ref. 180 with permission from John Wiley and Sons. (G) A wearable microneedle patch with a carbon nanotube biointerface for ISF cytokine detection. Reproduced from ref. 184 with permission from John Wiley and Sons. (H) A closed-loop platform for ocular surface inflammation (OSI) management. Reproduced from ref. 192 with permission from American Association for the Advancement of Science. (I) A wireless wearable patch for noninvasive, real-time and picomolar-level detection of CRP in sweat. Reproduced from ref. 171 with permission from Springer Nature.

In this section, we systematically review recent advances in wearable biosensors for protein detection, focusing on optical and electrical sensing approaches. Among electrical wearable biosensors, label-free techniques—particularly those utilizing electrochemical and FET mechanisms—have become increasingly dominant. In contrast, labeled approaches, including nanoparticle-based detection and sandwich immunoassays, are relatively less common in electrical systems. In optical wearable biosensors, label-free techniques remain prevalent due to their compatibility with wearable device requirements. However, labeled methods, such as sandwich immunoassays, still play a role in certain optical sensing applications. Similarly, highly efficient sampling strategies have been integrated into wearable protein biosensing devices, including spontaneous excretion, reverse iontophoresis, and stimulation-induced sampling.[172–174]

Label-free wearable electrical biosensors for protein detection

Wearable electrical sensors for protein detection, similar to metabolite sensors, commonly utilize a variety of device configurations, including three-electrode systems, capacitors, and FETs, as shown in Fig. 6A–F. These sensor configurations are highly effective for detecting specific proteins in biofluids such as sweat, ISF, and tears using multiple enhancing methods and integration strategies.

Fig. 6A illustrates the basic structure of a three-electrode system used for protein detection.[37] Typically, nanomaterials such as gold nanoparticles (AuNPs) are modified on the working electrode, along with affinity or active antibody molecules capable of specifically recognizing proteins. Upon binding, a change in the electrical signal occurs, enabling the quantitative analysis of protein molecules. Further modification and application of high-performance nanomaterials can promote enhanced sensitivity as shown in Fig. 6B. Jie Fu *et al.* employed a ZIF-67@AuNPs nanocomposite with a high surface area and conductivity to modify the working electrode, achieving excellent sensitivity and anti-interference performance.[175] Multiplexed monitoring can also be applied in wearable protein biosensors as shown in Fig. 6C. Yuji Gao *et al.* introduced VeCare, the first integrated wound monitoring platform designed for bedside use in chronic wounds such as venous ulcers.[31] This flexible immunosensing system allows multiplex detection of inflammatory biomarkers including TNF-α, IL-6, IL-8, and TGF-β1. A sawtooth-shaped capillary network (tapering from 200 to 160 μm) facilitates directional fluid transport, while aptamers modified with AuNPs–graphene enable minute-level, *in situ* detection of wound biomarkers. Recent advances have also demonstrated fully wearable platforms capable of real-time protein detection in undiluted sweat. For example, Huang *et al.* developed an ultra-flexible graphene field-effect transistor integrated with a Janus membrane (Fig. 6D) that enables automatic sweat collection and impurity filtering, allowing continuous and label-free monitoring of cytokines such as TNF-α directly on skin.[172]

Another widely used device configuration is the field-effect transistor (FET)-based sensor.[176–179] By modifying the gate with nanomaterials and aptamer molecules, a shift in the transfer curve or working curve occurs upon specific binding, which is then used for quantification, as shown in Fig. 6E and 7F. As shown in Fig. 6E, Huang *et al.* developed a highly deformable MoS_2 FET integrated with a nanosphere array capable of automatic sweat collection and impurity isolation, allowing direct quantification of TNF-α in undiluted sweat with a detection range of 10 fM–1 nM.[178] This ultrathin device maintains stable electrical performance under bending, folding, and crumpling, highlighting its strong potential for continuous, wearable cytokine monitoring. Similarly, Fig. 6F illustrates a comparable detection principle, employing PET as the flexible substrate.[180] Upon aptamer-protein binding, the G-quadruplex is formed, which induces changes in carrier concentration near the graphene, resulting in a specific signal variation.

Although proteins are abundantly present in blood, the invasive nature of blood sampling limits its suitability for continuous monitoring. ISF, which shares a highly similar protein composition with serum and plasma as confirmed by proteomic studies (*e.g.*, Bao Quoc Tran *et al.*),[181] offers a promising alternative. An increasing number of studies have demonstrated the feasibility of using microneedle-based platforms for ISF protein analysis.[182,183] For example, Jingxian Xu *et al.* developed a wearable microneedle patch with a carbon nanotube biointerface that integrates ISF sampling, cytokine capture (*via* immobilized antibodies), and electrochemical detection (Fig. 6G).[184] These developments collectively indicate that microneedle-assisted ISF sampling is becoming a powerful and rapidly expanding direction for minimally invasive, on-body protein monitoring.

Tear fluid also contains a variety of disease-associated proteins, including insulin-like growth factor-binding protein 3 (IGFBP3) and vascular endothelial growth factor (VEGF) for diabetes,[185–188] Aβ42 and tau protein for Alzheimer's disease,[189,190] and matrix metalloprotein-9 (MMP-9) and lactoferrin for dry eye syndrome.[191] These proteins offer valuable insights into disease onset and progression. Due to its non-invasive and easy accessibility, tear-based protein detection has become an important direction for wearable biosensors. However, challenges such as limited sample volume and low analyte concentration remain. Jiuk Jang *et al.* proposed a closed-loop platform for ocular surface inflammation (OSI) management, combining a graphene FET-based smart lens for wireless, real-time MMP-9 monitoring with a transparent, stretchable heating patch composed of Ag nanofiber networks (Fig. 6H).[192] Controlled *via* a smartphone, the patch delivers thermal therapy at 42 °C. With no electronics in the central lens area, visual clarity is maintained while enabling high-sensitivity OSI detection and treatment in a mobile health framework.

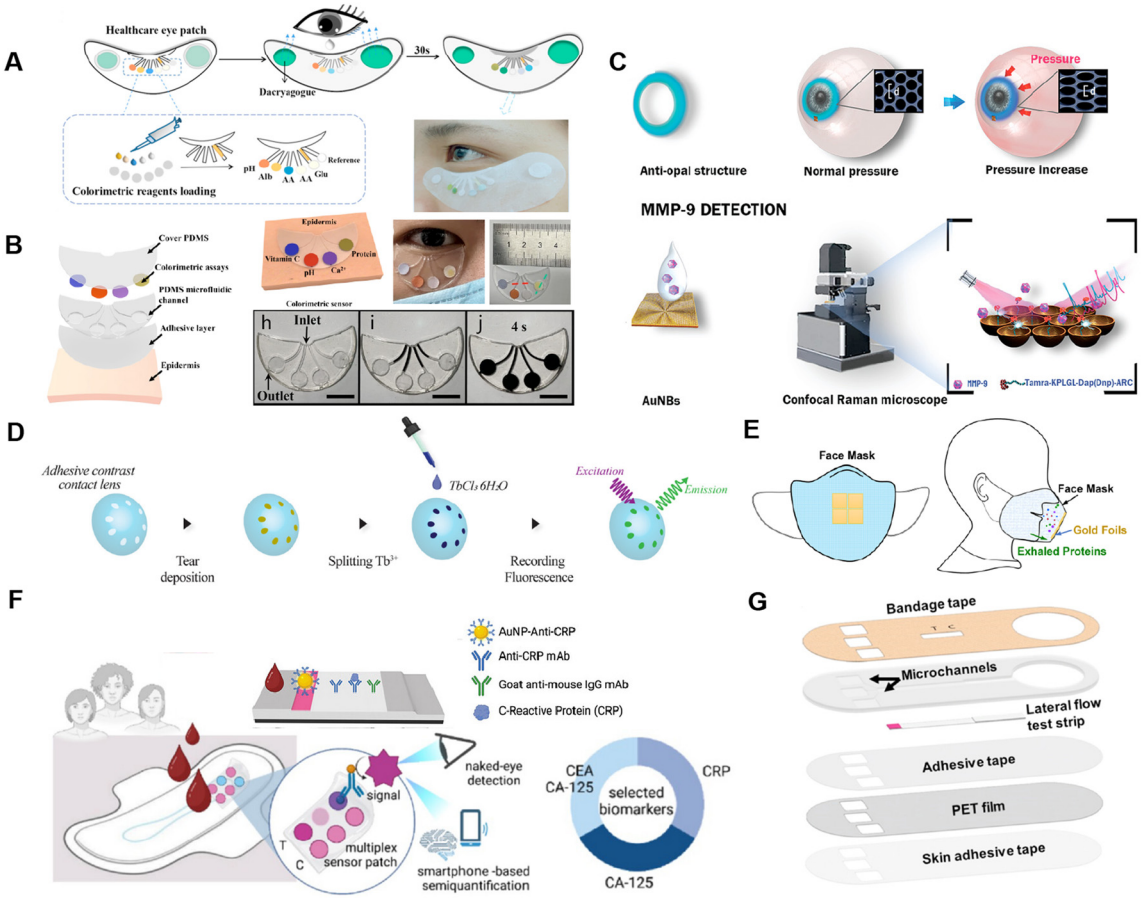

Fig. 7 Wearable biosensors for proteins in tear. (A) A non-invasive tear patch biosensor for detection of multiple analytes. Reproduced from ref. 33 with permission from American Chemical Society.[193] (B) An AI-integrated wearable system for rapid, non-invasive detection of tear protein. Reproduced from ref. 35 with permission under a Creative Commons CC BY license. (C) A dual-function lens platform based on optical sensing principles for MMP-9 detection. Reproduced from ref. 36 under a Creative Commons CC BY license. (D) A PDMS lens with selective adhesion properties. Reproduced from ref. 33 with permission from The Royal Society of Chemistry.[194] (E) Mask-integrated gold foil sampler, illustrating aerosol protein collection on the mask and subsequent elution, digestion, and nano-LC-MS/MS analysis for sensitive protein identification. Reproduced from ref. 33 with permission from John Wiley and Sons.[30] (F) A microfluidic detection platform for semi-quantitative detection of inflammatory, cancer, and endometriosis biomarkers. Reproduced from ref. 169 with permission under a Creative Commons CC BY license. (G) Integrating LFA with microneedle sampling for non-invasive detection of protein biomarkers in ISF. Reproduced from ref. 199 with permission under a Creative Commons CC BY license.

Labeled wearable electrical biosensors for protein detection

Compared to label-free approaches, labeled detection methods generally offer superior specificity and sensitivity, enabling reliable identification of target molecules within complex biological matrices. However, their typically high operational complexity poses challenges for integration into portable wearable sensors. Notably, some recent studies have addressed these limitations through innovative design strategies.

Jiaobing Tu *et al.* developed a wireless wearable patch named InflaStat, which represents the first system capable of noninvasive, real-time, picomolar-level CRP detection in sweat using labeled methods.[171] InflaStat integrates three main components: a sweat induction module utilizing iontophoresis and microfluidic channels, an electrochemical sensing module based on laser-engraved graphene (LEG) electrodes, and a flexible printed circuit for data acquisition and Bluetooth transmission (Fig. 6I). Together, they form a fully automated platform covering sweat collection, reagent mixing, and signal readout—marking a major milestone in continuous protein sensing *via* sweat. Elizabeth C. Wilkirson *et al.* developed a highly sensitive impedance sensor by combining AuNP–antibody complexes with IDEs for protein detection in ISF.[48] Upon binding to target proteins, the complexes altered the local dielectric constant, resulting in measurable impedance changes in the IDEs, achieving a detection limit as low as 1.33 pg mL^{-1}. In summary, wearable sensing strategies incorporating labels can significantly enhance detection sensitivity; however, they often require precise design and fabrication of microfluidic architectures—an aspect that is likely to define future development directions.

Label-free wearable optical biosensors for protein detection

Wearable optical sensors—primarily based on colorimetric, fluorescence, and surface-enhanced Raman scattering (SERS)

techniques—play an important role in protein detection. Various optical devices have been developed for the analysis of proteins in biofluids such as tears, exhaled breath, blood, and interstitial fluid. Due to the simplicity and portability required for wearable applications, most of these sensors adopt label-free detection strategies, which offer straightforward operation while maintaining adequate sensitivity for real-time health monitoring.

Jia Xu *et al.* developed a non-invasive tear patch biosensor composed of a multilayer structure, including a hydrophilic textile substrate, a sensing layer for colorimetric reactions, a tear secretion stimulant layer, and protective sealing layers (Fig. 7A).[193] This patch allows simultaneous detection of multiple analytes (pH, ascorbic acid, glucose, and protein), using the color change from bromophenol blue–protein binding, showing good sensitivity, selectivity, and anti-interference, making it suitable for home-based applications. To improve quantitative readouts of the colorimetric zones, Zihu Wang *et al.* proposed an AI-integrated wearable system (AI-WMCS) that combines flexible microfluidics with deep learning algorithms for rapid, non-invasive, and multiplex detection of vitamin C, pH, Ca^{2+}, and protein (Fig. 7B).[35] Constructed with PDMS, the system features four microchannels guiding tear fluid into circular chambers, requiring only 20 μL of tear volume and filling within 4 seconds. The cloud-based analysis platform (CSDAS), based on a CNN-GRU neural network, enables real-time prediction of biomarker concentrations with a detection limit down to 0.1 g L^{-1}.

Smart contact lenses have also gained attention for tear protein sensing. However, conventional designs face limitations such as reliance on electronic components, visual obstruction, and potential corneal damage. To overcome these issues, Ying Ye *et al.* introduced a dual-function lens platform based on optical sensing principles (Fig. 7C).[36] The lens monitors intraocular pressure (IOP) *via* a photonic crystal-based anti-opal structure, where pressure-induced lattice shifts lead to a visible blue shift in reflected light, enabling circuitry-free detection.

Simultaneously, Au nanobowl-based SERS substrates allow MMP-9 detection with a limit as low as 0.9 ng mL^{-1}. Aravind M. *et al.* addressed tear collection limitations by designing a PDMS lens with selective adhesion properties, enabling spontaneous tear separation without external force and enabling sensitive lactoferrin detection *via* fluorescence and colorimetry (Fig. 7D).[194]

Breath monitoring is also significant for disease diagnostics. Integrating biosensors into wearable face masks offers a promising noninvasive approach for disease diagnosis by detecting aerosolized proteins present in exhaled breath, using various optical sensing techniques. However, most exhaled proteins exist at extremely low concentrations, necessitating highly sensitive detection methods. To address this challenge, Shen-hui Cai *et al.* developed a mask-integrated gold foil adsorption array that serves as an efficient sampling platform for capturing aerosolized proteins. The collected proteins are subsequently eluted, enzymatically digested, and analyzed through nano-liquid chromatography tandem mass spectrometry (nano-LC-MS/MS). This workflow enables highly sensitive identification of exhaled aerosol proteins (Fig. 7E).[30]

Labeled wearable optical biosensors for protein detection

Labeled optical detection of proteins has shown great promise in enhancing the sensitivity of wearable biosensors, offering the potential for highly accurate and specific biomarker detection. By utilizing labels such as AuNP or enzymatic tags, these systems can amplify the signal, making it possible to detect even low-abundance proteins in complex biological samples. However, the integration of labelling agents introduces added complexity, both in terms of the required reagents and the need for more sophisticated detection equipment. As a result, only a limited number of studies have explored this approach in wearable biosensor development.

Lucas Dosnon *et al.* developed a microfluidic detection platform embedded in sanitary pads (MenstruAl) that enables semi-quantitative detection of inflammatory, cancer, and endometriosis biomarkers (CRP, CEA, CA-125) in menstrual blood using a fully instrument-free and visually readable LFA strip (Fig. 7F).[200] The system incorporates a dissolvable PVP membrane to precisely regulate a sample volume of 150 μL and a Fusion5 membrane to filter red blood cells, minimizing background noise. AI-enabled smartphone analysis further enhances automation and result interpretation. Elizabeth C. Wilkirson *et al.* integrated LFA with microneedle sampling to create a non-invasive wearable platform for detecting protein biomarkers in ISF (Fig. 7G).[199] ISF is passively delivered through microchannels into an LFIA strip without external actuation, enabling blood-free, rapid (<20 minutes), and equipment-free detection of biomarkers such as tetanus toxoid IgG and SARS-CoV-2 neutralizing antibodies.

In summary, proteins play vital roles in disease diagnosis and monitoring, and wearable biosensors offer a promising route for their non-invasive and continuous detection. This section highlights recent advances in the electrochemical or optical detection of key proteins, such as CRP, cytokines, MMP-9, and CEA in sweat, ISF, tears, and wound exudate using multiple microfluidic platforms. Some representative works are summarized in Table 2. Despite this progress, protein sensing in wearable formats remains constrained by limited sampling efficiency, low analyte concentrations, and the need for high sensitivity and specificity in complex biological matrices. To overcome these challenges, future efforts should focus on enhancing biomarker enrichment strategies, integrating multifunctional materials with signal amplification, and developing closed-loop systems for real-time monitoring and therapeutic intervention. Standardizing protein sensing protocols and validating clinical correlations

Table 2 Comparative analysis of wearable biosensors for protein sensing

Biofluid	Biomarkers	Sensing mechanism	Labeled or label-free	Material	Fabrication method	Ref
Sweat	CRP	Electrochemical	Labeled	PI, LEG, AuNPs, PET, hydrogels	Laser cutting	171
Sweat	CRP, cholesterol	Electrochemical	Label-free	LEG, ZIF-67@ AuNPs, GO-β-CD, PI, PET, PDMS	Screen printing, laser cutting	175
Sweat	IL-6	Electrochemical	Label-free	AuNPs, PET	Screen printing	37
Sweat	IFN-γ	FET	Label-free	Graphene, Nafion, Cr/Au, PET	Photolithography, E-beam deposition, CVD	180
Sweat	IL-1β, CRP	Electrochemical	Label-free	Gold, polymeric membrane	Screen printing	11
Sweat	IL-31, cortisol	Electrochemical	Label-free	PI, gold microelectrodes	Deposition, 3D printing	195, 196
Sweat	IL-6, IL-8, IL-10, TNF-α	Electrochemical	Label-free	Gold/zinc oxide, PI	Sputtering, deposition	197
Sweat	TNF-α	FET	Label-free	Graphene, PEN, Cr/Au, PDMS	Sputtering, CVD, photolithography, E-beam evaporation	198
Sweat	SARS-CoV-2	Inflammatory cytokines	Label-free	Graphene, PET, Cr/Au	CVD, photolithography, E-beam evaporation, 3-D printing	177
Exhaled breath	Proteins (*e.g.*, cytokeratins, cytokines)	Spectrum	Label-free	KN95, gold foil	Deposition	30
ISF	IL-6, TNF-α, IL-1β	Electrochemical	Label-free	Aminated CNT–chitosan, Au, PDMS	Sputtering, UV photolithography	184
ISF	IgG, SARS-CoV-2 antibodies	Colorimetric	Labeled	NC membrane, glass fiber, PMMA, PET	Soft lithography, laser cutting, LFIA assembly	199
ISF	CXCL9	Electrochemical	Labeled	Gold	Photolithography	48
Wound exudate	TNF-α, IL-6, IL-8, TGF-β1	Electrochemical	Label-free	Polyurethane, AuNPs, PET	Photolithography, evaporation, laser cutting	31
Tear	AA, albumin, glucose	Colorimetric	Label-free	Paper, textile fiber, wax, TBPB, GOx/HRP-TMB, DI, PMo, PDMS	Wax patterning, laser cutting	193
Tear	VC, proteins	Colorimetric	Label-free	DI, TBPB, PDMS, paper	Spin coating, laser cutting	35
Tear	MMP-9	SERS	Label-free	Poly(HEMA) hydrogel, AuNBs	Sputtering	36
Tear	MMP-9	Electrochemical	Label-free	AgNF, AgNW, Elastofilcon A, PI, PDMS, graphene	CVD, electrospinning	192
Blood	CRP, CEA, CA-125	Colorimetric	Labeled	AuNPs, paper	3D printing	200

LEG: laser-engraved graphene. CNT: carbon nanotube. NC: nitrocellulose. PMMA: poly(methyl methacrylate). LFIA: lateral flow immunochromatographic assay. AA: ascorbic acid. TBPB: tetrabromophenol blue. DI: 2,6-dichlorophenol indophenol. PMo: phosphomolybdic acid. CVD: chemical evaporation deposition. AgNF: silver nanofibers. AgNW: silver nanowires. IFN-γ: interferon-gamma. Nano-LC-MS/MS: nanoliquid chromatography-tandem mass spectrometry. AuNBs: gold nanobowls. Poly(HEMA): poly(2-hydroxyethyl methacrylate). CA: cancer antigen. CXCL9: C-X-C motif chemokine ligand 9.

will also be essential to advance wearable biosensors toward reliable, personalized healthcare applications.

Wearable nucleic acid biosensors

Nucleic acids (NA)—primarily DNA and RNA—are essential macromolecules that play a fundamental role in maintaining the normal physiological functions of living organisms. They are present in various biofluids, including blood, saliva, urine, exhaled breath, and sweat. In wearable biosensor systems, nucleic acids serve dual roles: as recognition probes[201] for the specific detection of biomolecules such as proteins, pathogens, and nucleic acids themselves, and as reporter elements[202] that transduce target-binding events into detectable signals.[203] Compared to traditional protein-based assays, nucleic acid molecules—particularly synthetically engineered ones—offer several notable advantages: they enable reagentless detection, exhibit high thermal stability, are easily and precisely modifiable, and possess programmable structural properties.[204,205] These features have driven the widespread adoption of nucleic acid-based strategies in wearable biosensing platforms, enabling highly sensitive and selective detection of target analytes.[206–208]

Despite the significant advantages of wearable nucleic acid sensing, its development is hindered by several critical challenges, primarily in three areas: effective sample collection, efficient nucleic acid amplification, and high-sensitivity signal detection. This section focuses on recent advances in non-invasive or minimally invasive detection of nucleic acid biomarkers using wearable technologies. Emphasis is placed on the detection of pathogenic nucleic acids (*e.g.*, viral DNA/RNA and bacterial DNA/RNA) and endogenous nucleic acids (*e.g.*, circulating tumour DNA (ctDNA), cell-free DNA (cfDNA), and microRNAs (miRNAs)), which hold significant clinical relevance for disease diagnosis and monitoring.

Sampling strategies in wearable nucleic acid biosensors

The concentration of nucleic acids in biofluids such as sweat, saliva, and tears is significantly lower than in blood, posing a

substantial challenge to sensor sensitivity. Moreover, extracted nucleic acids are highly prone to degradation, necessitating preservation of their integrity and stability throughout the processes of collection, transport, and detection. These constraints make the development of efficient, stable, and contamination-free sampling strategies particularly critical. In this regard, microfluidic structures play an essential role by enabling controlled routing, rapid

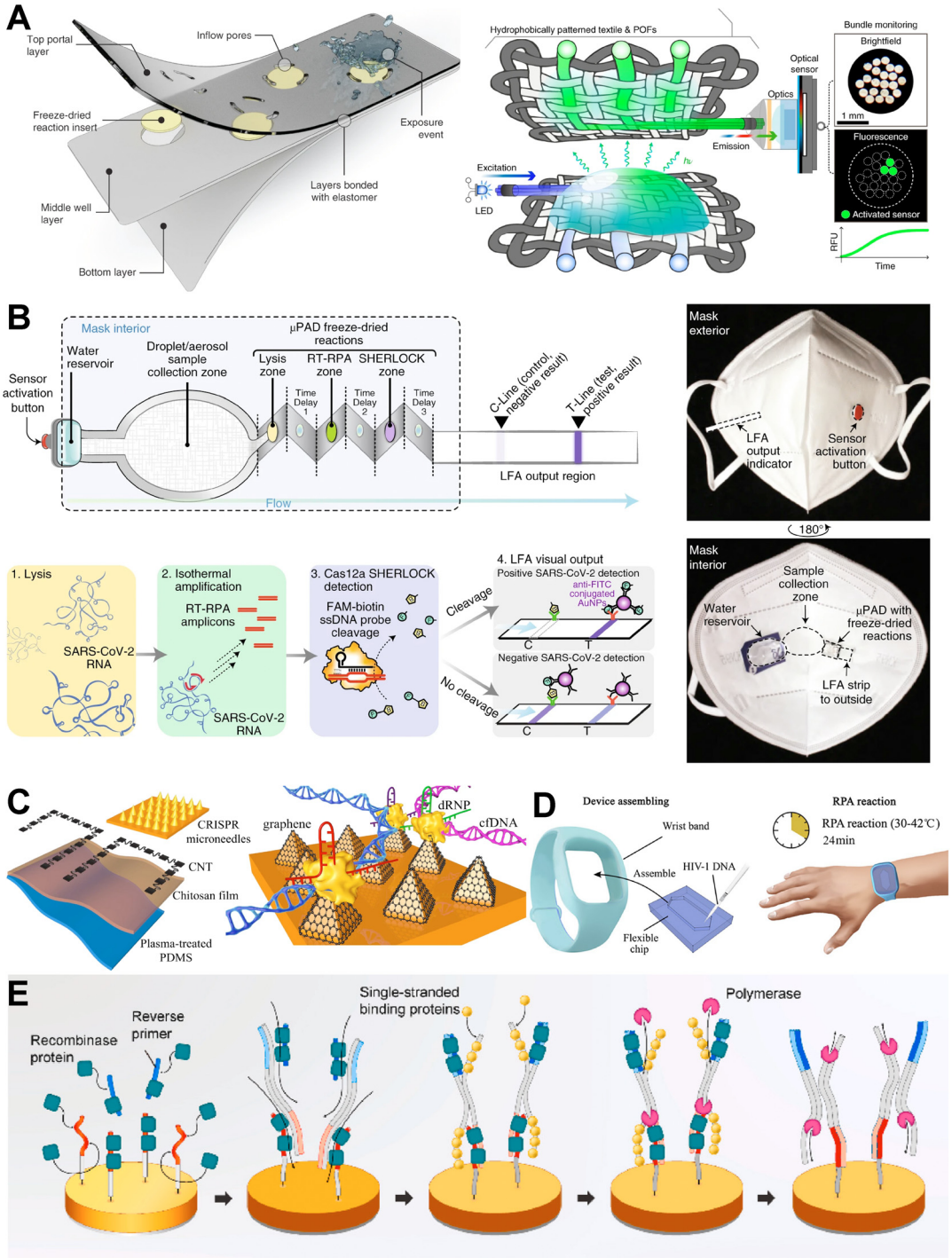

Fig. 8 NA sampling strategies used in wearable biosensors. (A) Lyophilized, cell-free synthetic biology biosensors integrated into lightweight, flexible substrates and textiles. Reproduced from ref. 209 with permission from Springer Nature. (B) A prototype facemask embedded with a freeze-dried CRISPR sensor for wearable COVID-19 diagnostics. Reproduced from ref. 209 with permission from Springer Nature. (C) Combination of reverse iontophoresis with hydrogel microneedles for improved ISF sampling efficiency when detecting low abundance NA. Reproduced from ref. 210 with permission under a Creative Commons CC BY license. (D) A wearable microfluidic device powered by body heat for RPA. Reproduced from ref. 211 with permission from Elsevier. (E) An electrochemical RPA biosensor that operates at human body temperature for highly sensitive detection of viral nucleic acids through on-chip isothermal amplification. Reproduced from ref. 213 with permission from Elsevier.

isolation, and protected transport of trace nucleic acids, helping to minimize degradation and external contamination. Consequently, establishing reliable microfluidic interfaces for non-invasive or minimally invasive acquisition of nucleic acid samples from the skin surface remains one of the key technical hurdles for wearable nucleic acid biosensing.

To address the difficulties of sampling and operational stability in wearable nucleic acid sensing, Peter Q. Nguyen and colleagues pioneered the development of lyophilized, cell-free synthetic biology biosensors integrated into lightweight, flexible substrates and textiles.[209] These systems operate without the need for invasive sampling or complex microfluidic pumps, instead relying on passive hydration activation and target molecule diffusion. Upon target recognition, the system can simultaneously generate a visible color change and a quantifiable fluorescence signal, wirelessly transmitted *via* optical fiber (Fig. 8A). The authors demonstrated a prototype facemask embedded with a freeze-dried CRISPR sensor for wearable COVID-19 diagnostics (Fig. 8B). Respiratory droplets from the wearer rehydrate and activate the embedded sensing elements; if viral nucleic acids (*e.g.*, SARS-CoV-2) are present, the system emits a detectable fluorescent signal, enabling noninvasive, real-time monitoring of health status and pathogen exposure.

To improve ISF sampling efficiency for low-abundance nucleic acid detection, Bin Yang *et al.* proposed a synergistic strategy combining reverse iontophoresis with hydrogel microneedles.[210] Furthermore, they developed an "on-line" detection system for continuous *in vivo* monitoring of circulating cfDNA. Unlike conventional methods involving offline extraction and laboratory analysis, this integrated microneedle array directly captures cfDNA from ISF using a CRISPR-functionalized tip (Fig. 8C). The captured nucleic acids are specifically recognized by CRISPR–Cas9, and the resulting molecular interaction is transduced into an electrical signal through a graphene-based bio-interface. This device streamlines the detection workflow and offers excellent sensitivity and specificity, representing a promising direction for future clinical applications.

Amplification strategies in wearable NA biosensors

Nucleic acid amplification techniques—including PCR, LAMP, RPA, and CRISPR-based methods—are fundamental to sensitive molecular diagnostics. While PCR remains the gold standard in laboratory settings, its reliance on thermal cycling renders it energy-intensive and thus less suitable for integration into wearable systems. In contrast, isothermal amplification methods such as LAMP (loop-mediated isothermal amplification) and RPA (recombinase polymerase amplification) offer more practical alternatives for wearable applications due to their operational simplicity and lower power requirements. However, the seamless integration of these techniques into miniaturized, resource-constrained wearable platforms—while maintaining high sensitivity and specificity—remains a significant engineering and biochemical challenge. Additionally, issues such as complex primer design and non-specific amplification continue to hinder robust performance in field-deployable systems.

Recent developments in nucleic acid diagnostics have begun shifting from benchtop POCT systems toward miniaturized, flexible platforms that are more compatible with future wearable integration. Kong *et al.* designed a soft PDMS-based microfluidic patch that performs recombinase polymerase amplification (RPA) using only human body heat (Fig. 8D), enabling electricity-free amplification of HIV-1 DNA with smartphone fluorescence readout (detection limit ≈ 100 copies per mL).[211] In parallel, Yang *et al.* developed a bandage-like wearable RPA microfluidic patch that utilizes human body heat (30–37 °C) to drive isothermal amplification and enables rapid, visual detection of nucleic acids on skin.[212] The flexible Ecoflex–PDMS structure conforms to various body locations and allows fluorescence-based readout of RPA amplicons within 10 min, demonstrating a practical pathway toward truly wearable nucleic acid diagnostics.

Complementing these optical approaches, Kim *et al.* developed an electrochemical RPA biosensor that operates at human body temperature and enables highly sensitive detection of viral nucleic acids through on-chip isothermal amplification coupled with differential pulse voltammetry (Fig. 8E).[213] The system achieves detection limits in the femtogram-per-microliter range for SARS-CoV-2 target genes, illustrating the potential of low-power electrochemical amplification modules for future wearable NA sensing. Together, these studies indicate a clear trend toward integrating sampling, amplification, and molecular readout within soft, low-power, and skin-compatible architectures—laying the foundation for next-generation wearable nucleic acid diagnostics.

Amplification-free strategies in wearable NA biosensors

In wearable nucleic acid diagnostics, amplification-free strategies enable the direct detection of target nucleic acids without relying on conventional amplification techniques such as PCR or RPA. These approaches improve sensitivity by enhancing signal output or minimizing background interference, making them particularly advantageous for resource-limited settings or applications requiring rapid response. Microfluidic enrichment and electrochemical amplification are commonly employed in these platforms.[13,214–216]

One promising technological route toward wearable nucleic acid detection is the integration of CRISPR systems. Hajian *et al.* immobilized catalytically deactivated Cas9 (dCas9) complexed with a sequence-specific sgRNA onto a graphene field-effect transistor, where the binding of target genomic DNA directly modulates the electrical characteristics of the graphene channel, enabling rapid (≈15 min) and highly sensitive (~1.7 fM) detection without nucleic acid

amplification.[38] Although the authors did not explore wearable applications, this amplification-free, near-single-molecule electrical readout mechanism is inherently compatible with flexible electronics, high-density microfluidics, and low-power readout circuits, and is therefore considered a highly promising direction for future wearable nucleic acid sensing.

Beyond CRISPR-based strategies, Wang *et al.* recently demonstrated an ultrahigh-sensitivity molecular electromechanical sensing (MoIEMS) platform that couples aptamer-functionalized tetrahedral DNA nanoprobes with a liquid-gated graphene FET to electrically detect ions, proteins, and unamplified nucleic acids.[14] By leveraging nanoscale electromechanical actuation and minimized Debye screening, the system achieves femtomolar- to attomolar-level detection and can identify SARS-CoV-2 RNA directly from clinical samples without amplification. Although currently demonstrated in a benchtop format, its compact g-FET architecture, low-voltage operation, and inherent compatibility with flexible substrates suggest strong potential for future translation into wearable nucleic acid sensing systems.

Wearable nucleic acid biosensors offer a promising approach for the non-invasive detection of clinically relevant DNA and RNA biomarkers, enabling early diagnosis and real-time monitoring of infectious and chronic diseases. Recent advances have demonstrated various sensing strategies based on CRISPR, graphene field-effect transistors, and microfluidic integration, along with innovative amplification methods such as isothermal amplification and amplification-free signal transduction. Despite these advancements, the development of wearable nucleic acid biosensors currently lags protein and metabolite detection, primarily due to inherent technical challenges in nucleic acid testing: complex amplification processes, single-molecule-level sensitivity requirements, and interference from complex biomatrix components. However, with breakthroughs in amplification-free detection technologies, this field is now at a turning point. These biosensors hold immense potential for real-time monitoring of respiratory viruses (*e.g.*, influenza, COVID-19), outbreak prevention, and early community transmission alerts. If challenges in sensing sensitivity, signal stability, and mass production can be addressed, such biosensors will become critical tools for large-scale infectious disease control, enabling molecular diagnostics to transition from laboratories to dynamic, personalized monitoring systems.

Comparative analysis of different sensing mechanisms

In recent years, wearable biosensors have achieved significant breakthroughs in health monitoring by enabling real-time and continuous tracking of various critical biomarkers. As summarized in Fig. 9, the sensing mechanisms used in wearable platforms can be broadly grouped into two main categories: electrical sensing and optical sensing. These two routes differ not only in how signals are generated and read out, but also in what types of targets they are best suited to detect and how well they support long-term on-body operation. In general, electrical approaches are particularly

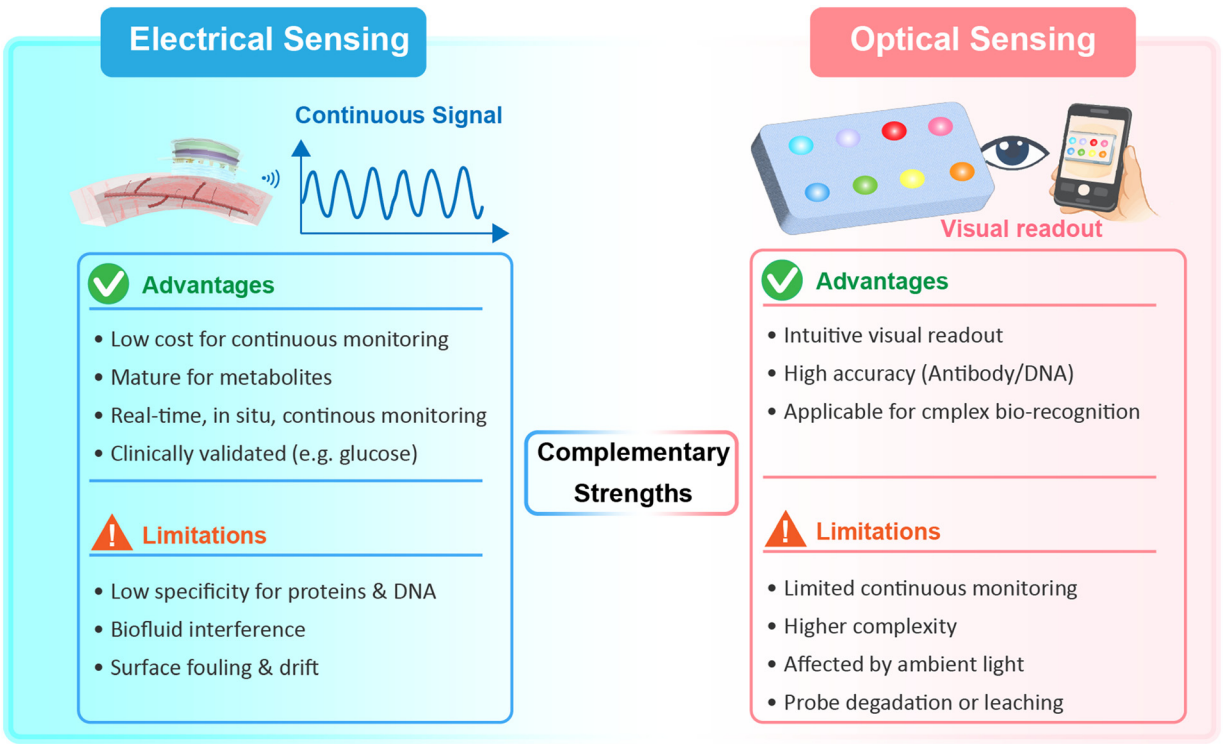

Fig. 9 Comparative advantages and limitations of electrical and optical wearable biosensing strategies.

strong in enabling continuous, high-temporal-resolution monitoring through direct electrical readouts, but in practice they are most mature and reliable for small-molecule metabolites. By contrast, optical approaches offer intuitive, visually interpretable signals and often benefit from highly specific recognition chemistries, yet they are typically less suitable for truly continuous monitoring on the body. These complementary strengths and limitations motivate a growing interest in hybrid designs that combine electrical and optical advantages, aiming to achieve multimodal, continuous health monitoring with improved robustness and interpretability.

Wearable electrical sensing: strengths and limitations

Electrical sensing methods, including electrochemical patches, FET-based detectors, and microneedle-enabled ISF extraction systems, represent one of the most mature and reliable technological routes in wearable biosensing. In metabolite monitoring, these platforms have demonstrated strong analytical performance, offering high sensitivity, fast response, and stable signal transduction that can be readily interfaced with low-power electronics. In particular, electrochemical glucose sensing has reached a high level of technological maturity, as evidenced by the widespread clinical adoption of commercial continuous glucose monitoring (CGM) devices, reflecting robust accuracy and user-level reliability.[217–220] Nevertheless, the advantages of electrical sensing are not universally transferable across analyte classes. For proteins and nucleic acids, continuous real-time monitoring remains challenging due to slower binding kinetics, limited availability of stable and selective recognition interfaces, and the need for signal amplification or multi-step assay formats. In addition, electrical signals can be susceptible to nonspecific adsorption and matrix effects from complex biofluids, leading to cross-interference, baseline drift, and compromised specificity without careful surface engineering and calibration strategies.

Wearable optical sensing: strengths and limitations

Optical sensing strategies offer a complementary pathway for wearable biosensing, with several distinct advantages and inherent limitations. A key strength of optical methods lies in the intuitive nature of optical signals, which can often be directly interpreted by the naked eye or simple imaging devices such as smartphone cameras, enabling low-cost and user-friendly readout. In addition, the use of highly specific recognition elements—such as antibody–antigen interactions or nucleic acid hybridization—confers excellent molecular selectivity, making optical platforms particularly well suited for protein and nucleic acid detection. These approaches also facilitate multiplexed analysis through spectral encoding or spatial patterning, allowing simultaneous monitoring of multiple analytes within a single device. However, optical sensing typically suffers from limited reliability and reproducibility under on-body conditions. Signal intensity can be strongly influenced by ambient lighting, optical path variations, probe leaching, and photobleaching, which complicate quantitative analysis. Moreover, many optical assays rely on accumulation-based or endpoint readouts, restricting their ability to provide continuous, real-time monitoring. These factors currently limit the long-term stability and robustness of optical wearable sensors, especially for extended use in dynamic physiological environments.

Overall, the strengths of electrical sensing in mature, quantitative metabolite monitoring and the strengths of optical sensing in specific, multiplexed biomolecular detection are highly complementary. Accordingly, next-generation wearable systems are increasingly moving toward hybrid, multimodal designs—often coupled with data processing/analytics—to improve robustness, interpretability, and clinical translatability.

Key challenges for wearable biosensing

Sample collection and stability

Sample collection is a major challenge for wearable biosensors, and the difficulties differ across biofluids. For sweat sensing, the main issues are unstable sweat production and flow rate, as well as channel blockage or residue buildup, which can reduce repeatability. For interstitial fluid (ISF), sampling is not fully noninvasive: minimally invasive methods such as microneedles may cause skin irritation and require careful safety validation, and the collected volume is usually small, which limits continuous testing. Saliva sensing is strongly affected by the oral environment, where food intake and daily activities can introduce large interference; saliva can also clog channels because of its complex composition. Tear sensing is even more difficult for long-term continuous sampling, and device contact may trigger reflex tearing and discomfort. For exhaled breath, the key limitation is that target analytes are often at very low concentrations, making stable detection difficult. Overall, these biofluid-specific challenges highlight the need for tailored sampling designs to achieve reliable wearable measurements.

To overcome these challenges, sampling and collection methods such as paper-based microfluidics, capillary bursting valves, and pump-driven systems have been extensively studied recently. A growing number of super-absorbent polymers and stimuli-responsive hydrogels are being researched and applied in sampling systems, showing great potential to further improve sampling efficiency. Meanwhile, to enhance the robustness of sampling, one-way valves and sealing structures are often employed to prevent backflow of samples or contamination from external air. In summary, achieving stable sampling and fluid-driven control relies heavily on ingenious physical structure design and the strategic application of functional materials.

Bio-interface stability under on-body conditions

Maintaining a reliable biotic–abiotic interface remains a major obstacle for both electrical and optical wearable sensors, as on-body conditions often induce electrode drift, fouling, reagent degradation, and optical interference. To address this issue, high-performance antifouling coatings, selective membranes, and flexible substrates have been integrated into the devices. Additionally, the incorporation of reference channels enables dynamic calibration and background subtraction, effectively mitigating baseline drift. These strategies collectively contribute to enhancing the interfacial reliability of wearable sensors.

Limited correlation with systemic physiology

In wearable biosensing, blood-based testing remains the clinical gold standard because it most directly reflects systemic physiology and provides well-established diagnostic thresholds. In contrast, for peripheral biofluids—such as interstitial fluid, sweat, tears, and saliva—the quantitative relationship to blood biomarkers is often not yet fully established and may vary with time, location, individual physiology, and sampling conditions. Differences in transport pathways, local tissue processes, secretion dynamics, and potential contamination can introduce delays and nonlinearity, making direct interpretation of wearable readouts more challenging. Addressing it requires a dual approach combining both engineering and clinical perspectives. Clinically, the focus should shift toward monitoring dynamic changes in biomarker concentrations and establishing correlations among multiple indicators. This can be complemented by invasive validation studies and synchronized animal experiments to build robust physiological correlations. On the engineering side, adopting multi-modal sensing strategies can yield richer datasets, which can then be processed using advanced data science and AI algorithms to extract meaningful insights from complex, noisy, and multi-dimensional data.[53,221,222]

Conclusion

Wearable biosensors are rapidly moving from proof-of-concept demonstrations toward practical health monitoring, yet key gaps remain in reliable sampling, long-term on-body stability, and the interpretation of signals across different biofluids. Building on the advances reviewed in this work across metabolites, proteins, and nucleic acids, future progress is expected to center on three directions. First, multimodal integration—combining electrical and optical readouts with physical parameters such as temperature, flow, and motion—can improve robustness and reduce drift in real-world use. Second, AI-driven analytics can help convert noisy, multi-source signals into actionable information, supporting individualized baselines and trend-based assessment rather than single-point readings. Third, systematic clinical validation and standardization are essential, including unified sampling protocols, clearer relationships between peripheral biofluids and blood, and longitudinal human studies. Together, these efforts will help translate wearable biofluid sensing from laboratory prototypes into reliable tools for disease screening, therapy support, and continuous health management.

Author contributions

Z. R. and Y. C. wrote the paper. Y. C. conceptualized the topic of this study.

Conflicts of interest

There are no conflicts to declare.

Data availability

No primary research results, software or code have been included and no new data were generated or analysed as part of this review.

Acknowledgements

The authors greatly acknowledge National Key R&D Program of China (No. 2022YFB3204400), Beijing Science and Technology Planning Project (No. Z251100004625024), National Natural Science Foundation of China (No. 52572310), and State Key Laboratory of Vascular Homeostasis and Remodeling of Peking University.

References

1 J. Min, J. Tu, C. Xu, H. Lukas, S. Shin, Y. Yang, S. A. Solomon, D. Mukasa and W. Gao, *Chem. Rev.*, 2023, **123**, 5049–5138.
2 N. Brasier, J. Wang, W. Gao, J. R. Sempionatto, C. Dincer, H. C. Ates, F. Güder, S. Olenik, I. Schauwecker, D. Schaffarczyk, E. Vayena, N. Ritz, M. Weisser, S. Mtenga, R. Ghaffari, J. A. Rogers and J. Goldhahn, *Nature*, 2024, **636**, 57–68.
3 S. Chen, Z. Qiao, Y. Niu, J. C. Yeo, Y. Liu, J. Qi, S. Fan, X. Liu, J. Y. Lee and C. T. Lim, *Nat. Rev. Bioeng.*, 2023, **1**, 950–971.
4 J. R. Sempionatto, M. Lin, L. Yin, E. De La Paz, K. Pei, T. Sonsa-Ard, A. N. De Loyola Silva, A. A. Khorshed, F. Zhang, N. Tostado, S. Xu and J. Wang, *Nat. Biomed. Eng.*, 2021, **5**, 737–748.
5 Q. Liu, Y. Liu, F. Wu, X. Cao, Z. Li, M. Alharbi, A. N. Abbas, M. R. Amer and C. Zhou, *ACS Nano*, 2018, **12**, 1170–1178.
6 Q. Zhang, D. Jiang, C. Xu, Y. Ge, X. Liu, Q. Wei, L. Huang, X. Ren, C. Wang and Y. Wang, *Sens. Actuators, B*, 2020, **320**, 128325.
7 Y. Yang, Y. Song, X. Bo, J. Min, O. S. Pak, L. Zhu, M. Wang, J. Tu, A. Kogan, H. Zhang, T. K. Hsiai, Z. Li and W. Gao, *Nat. Biotechnol.*, 2020, **38**, 217–224.
8 Y. Lei, W. Zhao, Y. Zhang, Q. Jiang, J. H. He, A. J. Baeumner, O. S. Wolfbeis, Z. L. Wang, K. N. Salama and H. N. Alshareef, *Small*, 2019, **15**, 1901190.

9 X. Luo, H. Yu and Y. Cui, *IEEE Electron Device Lett.*, 2018, **39**, 123–126.
10 A. Pal, D. Goswami, H. E. Cuellar, B. Castro, S. Kuang and R. V. Martinez, *Biosens. Bioelectron.*, 2018, **117**, 696–705.
11 B. Jagannath, K.-C. Lin, M. Pali, D. Sankhala, S. Muthukumar and S. Prasad, *Inflammatory Bowel Dis.*, 2020, **26**, 1533–1542.
12 H. C. Ates, P. Q. Nguyen, L. Gonzalez-Macia, E. Morales-Narváez, F. Güder, J. J. Collins and C. Dincer, *Nat. Rev. Mater.*, 2022, **7**, 887–907.
13 J.-H. Choi, J. Lim, M. Shin, S.-H. Paek and J.-W. Choi, *Nano Lett.*, 2020, **21**, 693–699.
14 L. Wang, X. Wang, Y. Wu, M. Guo, C. Gu, C. Dai, D. Kong, Y. Wang, C. Zhang, D. Qu, C. Fan, Y. Xie, Z. Zhu, Y. Liu and D. Wei, *Nat. Biomed. Eng.*, 2022, **6**, 276–285.
15 A. Erdem, E. Eksin, H. Senturk, E. Yildiz and M. Maral, *TrAC, Trends Anal. Chem.*, 2024, **171**, 117510.
16 W. Gao, S. Emaminejad, H. Y. Y. Nyein, S. Challa, K. Chen, A. Peck, H. M. Fahad, H. Ota, H. Shiraki, D. Kiriya, D.-H. Lien, G. A. Brooks, R. W. Davis and A. Javey, *Nature*, 2016, **529**, 509–514.
17 H. Y. Y. Nyein, L.-C. Tai, Q. P. Ngo, M. Chao, G. B. Zhang, W. Gao, M. Bariya, J. Bullock, H. Kim, H. M. Fahad and A. Javey, *ACS Sens.*, 2018, **3**, 944–952.
18 T. Laochai, J. Yukird, N. Promphet, J. Qin, O. Chailapakul and N. Rodthongkum, *Biosens. Bioelectron.*, 2022, **203**, 114039.
19 Y. Wang, C. Zhao, J. Wang, X. Luo, L. Xie, S. Zhan, J. Kim, X. Wang, X. Liu and Y. Ying, *Sci. Adv.*, 2021, **7**, eabe4553.
20 K. Liu, H. Wang, F. Zhu, Z. Chang, R. Du, Y. Deng and X. Qi, *ACS Nano*, 2024, **18**, 14207–14217.
21 F. Han, J. Li, P. Xiao, Y. Yang, H. Liu, Z. Wei, Y. He and F. Xu, *Biosens. Bioelectron.*, 2024, **257**, 116284.
22 M. Parrilla, A. Vanhooydonck, M. Johns, R. Watts and K. De Wael, *Sens. Actuators, B*, 2023, **378**, 133159.
23 S. Cho, C. Won, C. Kwon, H. Kim, S. Lee, K. Yoon, M. Lee, J. Kim, M. Lee, S. Lee, J. Lee, E. Song, Y. Mei, J. Lee and T. Lee, *ACS Sens.*, 2025, **10**, 148–158.
24 X. Li, C. Luo, Q. Fu, C. Zhou, M. Ruelas, Y. Wang, J. He, Y. Wang, Y. S. Zhang and J. Zhou, *Adv. Mater.*, 2020, **32**, 2000060.
25 X. Zheng, F. Zhang, K. Wang, W. Zhang, Y. Li, Y. Sun, X. Sun, C. Li, B. Dong, L. Wang and L. Xu, *TrAC, Trends Anal. Chem.*, 2021, **140**, 116281.
26 B. Sarac, S. Yücer, H. Sahin, M. Unal and F. Ciftci, *Chem. Eng. J.*, 2024, **491**, 152016.
27 W. Liu, Z. Du, Z. Duan, L. Li and G. Shen, *Nat. Commun.*, 2024, **15**, 5635.
28 Z. Duan, M. Yuan, Z. Liu, W. Pei, K. Jiang, L. Li and G. Shen, *Small*, 2024, **20**, 2309785.
29 W. Heng, S. Yin, J. Min, C. Wang, H. Han, E. Shirzaei Sani, J. Li, Y. Song, H. B. Rossiter and W. Gao, *Science*, 2024, **385**, 954–961.
30 S. H. Cai, B. Wang, J. Zhang, J. Guo and B. Hu, *Rapid Commun. Mass Spectrom.*, 2024, **38**, 9737.
31 Y. Gao, D. T. Nguyen, T. Yeo, S. B. Lim, W. X. Tan, L. E. Madden, L. Jin, J. Y. K. Long, F. A. B. Aloweni, Y. J. A. Liew, M. L. L. Tan, S. Y. Ang, S. D. O. Maniya, I. Abdelwahab, K. P. Loh, C.-H. Chen, D. L. Becker, D. Leavesley, J. S. Ho and C. T. Lim, *Sci. Adv.*, 2021, **7**, eabg9614.
32 Y. Yao, J. Chen, Y. Guo, T. Lv, Z. Chen, N. Li, S. Cao, B. Chen and T. Chen, *Biosens. Bioelectron.*, 2021, **179**, 113078.
33 T. Abbasiasl, F. Mirlou, H. Mirzajani, M. J. Bathaei, E. Istif, N. Shomalizadeh, R. E. Cebecioğlu, E. E. Özkahraman, U. C. Yener and L. Beker, *Adv. Mater.*, 2024, **36**, 2304704.
34 Z. Chen, Y. Guo, X. Gu, X. Liu, J. Zhang, C. Song and L. Wang, *Microchem. J.*, 2024, **206**, 111546.
35 Z. Wang, Y. Dong, X. Sui, X. Shao, K. Li, H. Zhang, Z. Xu and D. Zhang, *npj Flexible Electron.*, 2024, **8**, 35.
36 Y. Ye, Y. Ge, Q. Zhang, M. Yuan, Y. Cai, K. Li, Y. Li, R. Xie, C. Xu, D. Jiang, J. Qu, X. Liu and Y. Wang, *Adv. Sci.*, 2022, **9**, 2104738.
37 M. Ploner, B. Shkodra, A. Altana, M. Petrelli, A. Tagliaferri, D. Resnati, P. Lugli, M. A. C. Angeli and L. Petti, *IEEE Sens. Lett.*, 2024, **8**, 1–4.
38 R. Hajian, S. Balderston, T. Tran, T. deBoer, J. Etienne, M. Sandhu, N. A. Wauford, J.-Y. Chung, J. Nokes, M. Athaiya, J. Paredes, R. Peytavi, B. Goldsmith, N. Murthy, I. M. Conboy and K. Aran, *Nat. Biomed. Eng.*, 2019, **3**, 427–437.
39 Y. Li, Y. Guo, H. Chen, X. Xiao, F. Long, H. Zhong, K. Wang, Z. Guo, Z. Zhuang and Z. Liu, *ACS Photonics*, 2024, **11**, 613–625.
40 N. Mishra, N. T. Garland, K. A. Hewett, M. Shamsi, M. D. Dickey and A. J. Bandodkar, *ACS Sens.*, 2022, **7**, 3169–3180.
41 H. Wu, J. Chen, P. Lin, Y. Su, H. Li, W. Xiao and J. Peng, *ACS Appl. Mater. Interfaces*, 2024, **16**, 39857–39866.
42 C. Ye, M. Wang, J. Min, R. Y. Tay, H. Lukas, J. R. Sempionatto, J. Li, C. Xu and W. Gao, *Nat. Nanotechnol.*, 2024, **19**, 330–337.
43 Á. Molinero-Fernandez, Q. Wang, X. Xuan, Å. Konradsson-Geuken, G. A. Crespo and M. Cuartero, *ACS Sens.*, 2024, **9**, 361–370.
44 C. Moonla, M. Reynoso, A. Casanova, A.-Y. Chang, O. Djassemi, A. Balaje, A. Abbas, Z. Li, K. Mahato and J. Wang, *ACS Sens.*, 2024, **9**, 1004–1013.
45 Q. Wang, Á. Molinero-Fernandez, Q. Wei, X. Xuan, Å. Konradsson-Geuken, M. Cuartero and G. A. Crespo, *ACS Sens.*, 2024, **9**, 3115–3125.
46 L. Li, Y. Zhou, C. Sun, Z. Zhou, J. Zhang, Y. Xu, X. Xiao, H. Deng, Y. Zhong, G. Li, Z. Chen, W. Deng, X. Hu and Y. Wang, *Acta Biomater.*, 2024, **175**, 199–213.
47 M.-J. Deng and Y.-S. Wu, *J. Alloys Compd.*, 2023, **945**, 169285.
48 E. C. Wilkison, Y. Gong, W. Li and P. B. Lillehoj, *2024 IEEE 37th International Conference on Micro Electro Mechanical Systems (MEMS)*, Austin, TX, USA, 2024.
49 B. Wang, C. Zhao, Z. Wang, K.-A. Yang, X. Cheng, W. Liu, W. Yu, S. Lin, Y. Zhao, K. M. Cheung, H. Lin, H. Hojaiji, P. S. Weiss, M. N. Stojanović, A. J. Tomiyama, A. M. Andrews and S. Emaminejad, *Sci. Adv.*, 2022, **8**, eabk0967.
50 X. Mei, J. Yang, J. Liu and Y. Li, *Chem. Eng. J.*, 2023, **454**, 140248.
51 Y. Wu, X. Li, K. E. Madsen, H. Zhang, S. Cho, R. Song, R. F. Nuxoll, Y. Xiong, J. Liu, J. Feng, T. Yang, K. Zhang, A. J.

Aranyosi, D. E. Wright, R. Ghaffari, Y. Huang, R. G. Nuzzo and J. A. Rogers, *Lab Chip*, 2024, **24**, 4288–4295.
52 R. Ghaffari, J. Choi, M. S. Raj, S. Chen, S. P. Lee, J. T. Reeder, A. J. Aranyosi, A. Leech, W. Li, S. Schon, J. B. Model and J. A. Rogers, *Adv. Funct. Mater.*, 2020, **30**, 1907269.
53 L. Zhou, S. S. Menon, X. Li, M. Zhang and M. H. Malakooti, *Adv. Mater. Technol.*, 2025, **10**, 2401121.
54 M. Deng, G. Song, K. Zhong, Z. Wang, X. Xia and Y. Tian, *Sens. Actuators, B*, 2022, **352**, 131067.
55 X.-Y. Xu and B. Yan, *J. Mater. Chem. C*, 2018, **6**, 1863–1869.
56 Y. Sekine, S. B. Kim, Y. Zhang, A. J. Bandodkar, S. Xu, J. Choi, M. Irie, T. R. Ray, P. Kohli, N. Kozai, T. Sugita, Y. Wu, K. Lee, K.-T. Lee, R. Ghaffari and J. A. Rogers, *Lab Chip*, 2018, **18**, 2178–2186.
57 L. Xia and G. Li, *J. Sep. Sci.*, 2021, **44**, 1752–1768.
58 C. Westley, Y. Xu, B. Thilaganathan, A. J. Carnell, N. J. Turner and R. Goodacre, *Anal. Chem.*, 2017, **89**, 2472–2477.
59 M. Saqib, L. Qi, P. Hui, A. Nsabimana, M. I. Halawa, W. Zhang and G. Xu, *Biosens. Bioelectron.*, 2018, **99**, 519–524.
60 R. Yang, W. Dong, Y. Ren, Y. Xue and H. Cui, *Anal. Chim. Acta*, 2022, **1220**, 340070.
61 H. Jin, Z. Zheng, Z. Cui, Y. Jiang, G. Chen, W. Li, Z. Wang, J. Wang, C. Yang, W. Song, X. Chen and Y. Zheng, *Nat. Commun.*, 2023, **14**, 4692.
62 Y. Chen, S. Hu, C. Shen, L. Zhang, C. Yi, Y. Chen, G.-S. Liu, L. Chen, Z. Chen and Y. Luo, *Nano Lett.*, 2025, **25**, 129–137.
63 V. Kansay, V. Dutt Sharma, V. Srivastava, N. Batra, S. Chakrabarti and M. K. Bera, *Microchem. J.*, 2024, **201**, 110624.
64 Y. Jung, M. Kim, S. Jeong, S. Hong and S. H. Ko, *ACS Nano*, 2024, **18**, 2312–2324.
65 T. Saha, S. Mukherjee, M. D. Dickey and O. D. Velev, *Lab Chip*, 2024, **24**, 1244–1265.
66 M. Parrilla, U. Detamornrat, J. Domínguez-Robles, S. Tunca, R. F. Donnelly and K. De Wael, *ACS Sens.*, 2023, **8**, 4161–4170.
67 Y. Wu, F. Tehrani, H. Teymourian, J. Mack, A. Shaver, M. Reynoso, J. Kavner, N. Huang, A. Furmidge, A. Duvvuri, Y. Nie, L. M. Laffel, F. J. Doyle, M.-E. Patti, E. Dassau, J. Wang and N. Arroyo-Currás, *Anal. Chem.*, 2022, **94**, 8335–8345.
68 M. Dervisevic, L. Esser, Y. Chen, M. Alba, B. Prieto-Simon and N. H. Voelcker, *Biosens. Bioelectron.*, 2025, **271**, 116995.
69 Z. Xu, X. Qiao, R. Tao, Y. Li, S. Zhao, Y. Cai and X. Luo, *Biosens. Bioelectron.*, 2023, **234**, 115360.
70 J. T. Reeder, Y. Xue, D. Franklin, Y. Deng, J. Choi, O. Prado, R. Kim, C. Liu, J. Hanson, J. Ciraldo, A. J. Bandodkar, S. Krishnan, A. Johnson, E. Patnaude, R. Avila, Y. Huang and J. A. Rogers, *Nat. Commun.*, 2019, **10**, 5513.
71 S. Guan, Y. Yang, Y. Wang, X. Zhu, D. Ye, R. Chen and Q. Liao, *Adv. Mater.*, 2024, **36**, 2305854.
72 L. Chen, M. Ren, J. Zhou, X. Zhou, F. Liu, J. Di, P. Xue, C. Li, Q. Li, Y. Li, L. Wei and Q. Zhang, *Proc. Natl. Acad. Sci. U. S. A.*, 2024, **121**, 2407971121.
73 H. H. Shi, Y. Pan, L. Xu, X. Feng, W. Wang, P. Potluri, L. Hu, T. Hasan and Y. Y. S. Huang, *Nat. Mater.*, 2023, **22**, 1294–1303.
74 Y. Wei, X. Shi, Z. Yao, J. Zhi, L. Hu, R. Yan, C. Shi, H.-D. Yu and W. Huang, *npj Flexible Electron.*, 2023, **7**, 13.
75 H. Liu, Q. Zhang, N. Yang, X. Jiang, F. Wang, X. Yan, X. Zhang, Y. Zhao and T. Cheng, *ACS Appl. Mater. Interfaces*, 2023, **15**, 44554–44562.
76 Y. Jiang, A. A. Trotsyuk, S. Niu, D. Henn, K. Chen, C.-C. Shih, M. R. Larson, A. M. Mermin-Bunnell, S. Mittal, J.-C. Lai, A. Saberi, E. Beard, S. Jing, D. Zhong, S. R. Steele, K. Sun, T. Jain, E. Zhao, C. R. Neimeth, W. G. Viana, J. Tang, D. Sivaraj, J. Padmanabhan, M. Rodrigues, D. P. Perrault, A. Chattopadhyay, Z. N. Maan, M. C. Leeolou, C. A. Bonham, S. H. Kwon, H. C. Kussie, K. S. Fischer, G. Gurusankar, K. Liang, K. Zhang, R. Nag, M. P. Snyder, M. Januszyk, G. C. Gurtner and Z. Bao, *Nat. Biotechnol.*, 2023, **41**, 652–662.
77 H. Y. Y. Nyein, M. Bariya, B. Tran, C. H. Ahn, B. J. Brown, W. Ji, N. Davis and A. Javey, *Nat. Commun.*, 2021, **12**, 1823.
78 J. Shao, X. Chen, X. Li, H. Tian, C. Wang and B. Lu, *Sci. China: Technol. Sci.*, 2019, **62**, 175–198.
79 A. Kalkal, S. Kumar, P. Kumar, R. Pradhan, M. Willander, G. Packirisamy, S. Kumar and B. D. Malhotra, *Addit. Manuf.*, 2021, **46**, 102088.
80 M. Dervisevic, M. J. Jara Fornerod, J. Harberts, P. S. Zangabad and N. H. Voelcker, *ACS Sens.*, 2024, **9**, 932–941.
81 B. Paul Kunnel and S. Demuru, *Lab Chip*, 2022, **22**, 1793–1804.
82 M. Wang, C. Ye, Y. Yang, D. Mukasa, C. Wang, C. Xu, J. Min, S. A. Solomon, J. Tu, G. Shen, S. Tang, T. K. Hsiai, Z. Li, J. S. McCune and W. Gao, *Nat. Mater.*, 2025, 589–598.
83 S. Henry, D. V. McAllister, M. G. Allen and M. R. Prausnitz, *J. Pharm. Sci.*, 1998, **87**, 922–925.
84 H. Y. Y. Nyein, W. Gao, Z. Shahpar, S. Emaminejad, S. Challa, K. Chen, H. M. Fahad, L.-C. Tai, H. Ota, R. W. Davis and A. Javey, *ACS Nano*, 2016, **10**, 7216–7224.
85 Z. Faraji Rad, P. D. Prewett and G. J. Davies, *Microsyst. Nanoeng.*, 2021, **7**, 71.
86 C. Zhao, D. Liu, Z. Cai, B. Du, M. Zou, S. Tang, B. Li, C. Xiong, P. Ji, L. Zhang, Y. Gong, G. Xu, C. Liao and Y. Wang, *Biosensors*, 2022, **12**, 71.
87 Y. Xue, Z. Weng, Q. Xiang, N. Liao and W. Xue, *Ceram. Int.*, 2024, **50**, 51429–51436.
88 M. A. Fraga, M. Massi and R. S. Pessoa, *IEEE Sens. J.*, 2024, **24**, 28–39.
89 Y. Liu, Q. Yu, X. Luo, L. Ye, L. Yang and Y. Cui, *Research*, 2022, **2022**, 9870637.
90 X. Li, X. Huang, J. Mo, H. Wang, Q. Huang, C. Yang, T. Zhang, H. J. Chen, T. Hang, F. Liu, L. Jiang, Q. Wu, H. Li, N. Hu and X. Xie, *Adv. Sci.*, 2021, **8**, 2100827.
91 T. Saha, R. Del Caño, K. Mahato, E. De la Paz, C. Chen, S. Ding, L. Yin and J. Wang, *Chem. Rev.*, 2023, **123**, 7854–7889.
92 F. Tehrani, H. Teymourian, B. Wuerstle, J. Kavner, R. Patel, A. Furmidge, R. Aghavali, H. Hosseini-Toudeshki, C. Brown, F. Zhang, K. Mahato, Z. Li, A. Barfidokht, L. Yin, P. Warren, N. Huang, Z. Patel, P. P. Mercier and J. Wang, *Nat. Biomed. Eng.*, 2022, **6**, 1214–1224.

93 C. Xu, Y. Song, J. R. Sempionatto, S. A. Solomon, Y. Yu, H. Y. Y. Nyein, R. Y. Tay, J. Li, W. Heng, J. Min, A. Lao, T. K. Hsiai, J. A. Sumner and W. Gao, *Nat. Electron.*, 2024, **7**, 168–179.
94 J. R. Sempionatto, J. A. Lasalde-Ramírez, K. Mahato, J. Wang and W. Gao, *Nat. Rev. Chem.*, 2022, **6**, 899–915.
95 Y. Cao, H. Shi, C. Yi, Y. Zheng, Z. Tan, X. Jia and Z. Liu, *TrAC, Trends Anal. Chem.*, 2024, **172**, 117561.
96 R. Song, S. Cho, S. Khan, I. Park and W. Gao, *Adv. Mater.*, 2025, 2419161.
97 N. Kashaninejad and N.-T. Nguyen, *Lab Chip*, 2023, **23**, 913–937.
98 A. Childs, B. Mayol, J. A. Lasalde-Ramírez, Y. Song, J. R. Sempionatto and W. Gao, *ACS Nano*, 2024, **18**, 24605–24616.
99 C.-B. Ma, X. Shang, M. Sun, X. Bo, J. Bai, Y. Du and M. Zhou, *ACS Sens.*, 2025, **10**, 2388–2408.
100 F. Ju, Y. Wang, B. Yin, M. Zhao, Y. Zhang, Y. Gong and C. Jiao, *Micromachines*, 2023, **14**, 1792.
101 S. Li, Z. Ma, Z. Cao, L. Pan and Y. Shi, *Small*, 2019, **16**, 1903822.
102 Y. Sun, X. Guo, Y. Jiang, J. Cui, J. Wu, J. Wang, W. Cheng, Y. Shi and L. Pan, *Analyst*, 2025, **150**, 4470–4489.
103 F. Bakhshandeh, H. Zheng, N. G. Barra, S. Sadeghzadeh, I. Ausri, P. Sen, F. Keyvani, F. Rahman, J. Quadrilatero, J. Liu, J. D. Schertzer, L. Soleymani and M. Poudineh, *Adv. Mater.*, 2024, **36**, 2313743.
104 D. L. B. Jing, X. Tian, Y. Wang, B. Cui, Y. Yang, S. Dai, W. Lin, J. Zhu, J. Wang, A. Xu, Z. Gu and S. Zhang, *Sci. Adv.*, 2024, **10**, eadl1856.
105 J. Zhao, Y. Lin, J. Wu, H. Y. Y. Nyein, M. Bariya, L.-C. Tai, M. Chao, W. Ji, G. Zhang, Z. Fan and A. Javey, *ACS Sens.*, 2019, **4**, 1925–1933.
106 Y. Liu, X. Luo, Y. Dong, M. Hui, L. Xu, H. Li, J. Lv, L. Yang and Y. Cui, *Anal. Chim. Acta*, 2022, **1227**, 340264.
107 H. Zhao, E. Su, L. Huang, Y. Zai, Y. Liu, Z. Chen, S. Li, L. Jin, Y. Deng and N. He, *Chin. Chem. Lett.*, 2022, **33**, 743–746.
108 T. Arakawa, K. Tomoto, H. Nitta, K. Toma, S. Takeuchi, T. Sekita, S. Minakuchi and K. Mitsubayashi, *Anal. Chem.*, 2020, **92**, 12201–12207.
109 M. Elsherif, F. Alam, A. E. Salih, B. Alqattan, A. K. Yetisen and H. Butt, *Small*, 2021, **17**, 2102876.
110 Y. Zhao, Q. Zhai, D. Dong, T. An, S. Gong, Q. Shi and W. Cheng, *Anal. Chem.*, 2019, **91**, 6569–6576.
111 J. Ma, Y. Jiang, L. Shen, H. Ma, T. Sun, F. Lv, A. Kiran and N. Zhu, *Biosens. Bioelectron.*, 2019, **144**, 111637.
112 X. Zhu, Y. Ju, J. Chen, D. Liu and H. Liu, *ACS Sens.*, 2018, **3**, 1135–1141.
113 X. Zhu, S. Yuan, Y. Ju, J. Yang, C. Zhao and H. Liu, *Anal. Chem.*, 2019, **91**, 10764–10771.
114 S. K. Kim, G. H. Lee, C. Jeon, H. H. Han, S. J. Kim, J. W. Mok, C. K. Joo, S. Shin, J. Y. Sim, D. Myung, Z. Bao and S. K. Hahn, *Adv. Mater.*, 2022, **34**, 2110536.
115 D. Lu, H. Li, N. Xiao, M. Jiang, Y. Zuna, S. Feng, Z. Li, J. Long, J. L. Marty and Z. Zhu, *Talanta*, 2025, **283**, 127197.
116 H. Lee, T. K. Choi, Y. B. Lee, H. R. Cho, R. Ghaffari, L. Wang, H. J. Choi, T. D. Chung, N. Lu, T. Hyeon, S. H. Choi and D.-H. Kim, *Nat. Nanotechnol.*, 2016, **11**, 566–572.
117 V. Lopes, T. Abreu, M. Abrantes, S. S. Nemala, F. De Boni, M. Prato, P. Alpuim and A. Capasso, *J. Am. Chem. Soc.*, 2025, **147**, 13059–13070.
118 Y. Zhang, Q. Huang, Z.-H. Sun, R. Zheng, Y. Ma, D. Han and L. Niu, *Anal. Chem.*, 2024, **96**, 18239–18245.
119 Y. Zhang, X. Zeng, C. Wang, Y. Liu, C. Jin, J. Chen, J. Hou, D. Huo and C. Hou, *Talanta*, 2025, **285**, 127404.
120 Y. Zhang, C. Jin, C. Wang, X. Zeng, M. Yang, C. Hou and D. Huo, *Biosens. Bioelectron.*, 2025, **271**, 117001.
121 F. Chen, J. Wang, L. Chen, H. Lin, D. Han, Y. Bao, W. Wang and L. Niu, *Anal. Chem.*, 2024, **96**, 3914–3924.
122 E. De la Paz, T. Saha, R. Del Caño, S. Seker, N. Kshirsagar and J. Wang, *Talanta*, 2023, **254**, 124122.
123 Y. Cheng, X. Gong, J. Yang, G. Zheng, Y. Zheng, Y. Li, Y. Xu, G. Nie, X. Xie, M. Chen, C. Yi and L. Jiang, *Biosens. Bioelectron.*, 2022, **203**, 114026.
124 G. Liu, X. Dou, P. Zhang, S. Yin, Q. Tan, X. Jin, C. Li and X. Zhang, *Talanta*, 2025, **293**, 128101.
125 J. Niu, S. Lin, D. Chen, Z. Wang, C. Cao, A. Gao, S. Cui, Y. Liu, Y. Hong, X. Zhi and D. Cui, *Small*, 2023, **20**, 2306769.
126 S. Ding, T. Saha, L. Yin, R. Liu, M. I. Khan, A.-Y. Chang, H. Lee, H. Zhao, Y. Liu, A. S. Nazemi, J. Zhou, C. Chen, Z. Li, C. Zhang, S. Earney, S. Tang, O. Djassemi, X. Chen, M. Lin, S. S. Sandhu, J.-M. Moon, C. Moonla, P. Nandhakumar, Y. Park, K. Mahato, S. Xu and J. Wang, *Nat. Electron.*, 2024, **7**, 788–799.
127 S. Zhang, H. Wang, Y. Zheng, Y. Yao, T. Li, Y. Ma, Y. Zhou, Z. Chen, Y. Wei, L. Fang, X. Chen, X. Ye, J. Zhou and B. Liang, *Adv. Funct. Mater.*, 2025, 2501970.
128 Q. Yuan, H. Fang, X. Wu, J. Wu, X. Luo, R. Peng, S. Xu and S. Yan, *ACS Appl. Mater. Interfaces*, 2023, **16**, 66810–66818.
129 Z. Zhang, M. Azizi, M. Lee, P. Davidowsky, P. Lawrence and A. Abbaspourrad, *Lab Chip*, 2019, **19**, 3448–3460.
130 X. Huang, C. Yao, S. Huang, S. Zheng, Z. Liu, J. Liu, J. Wang, H.-J. Chen and X. Xie, *ACS Sens.*, 2024, **9**, 1065–1088.
131 J. E. Lee, B. Sridharan, D. Kim, Y. Sung, J. H. Park and H. G. Lim, *Clin. Chim. Acta*, 2025, **575**, 120358.
132 J. Hanna, M. Bteich, Y. Tawk, A. H. Ramadan, B. Dia, F. A. Asadallah, A. Eid, R. Kanj, J. Costantine and A. A. Eid, *Sci Adv.*, 2020, **6**, eaba5320.
133 B. Hu, X. Kang, S. Xu, J. Zhu, L. Yang and C. Jiang, *Anal. Chem.*, 2023, **95**, 3587–3595.
134 B. Somchob, N. Passornraprasit, V. P. Hoven and N. Rodthongkum, *Microchim. Acta*, 2025, **192**, 204.
135 X. Mei, J. Yang, X. Yu, Z. Peng, G. Zhang and Y. Li, *Sens. Actuators, B*, 2023, **381**, 133451.
136 A. Pors, B. Korzeniowska, M. T. Rasmussen, C. V. Lorenzen, K. G. Rasmussen, R. Inglev, A. Philipps, E. Zschornack, G. Freckmann, A. Weber and K. D. Hepp, *Sci. Rep.*, 2025, **15**, 10226.
137 Y. Zhang, L. Zhang, L. Wang, S. Shao, B. Tao, C. Hu, Y. Chen, Y. Shen, X. Zhang, S. Pan, H. Cao, M. Sun, J. Shi, C.

Jiang, M. Chen, L. Zhou, G. Ning, C. Chen and W. Wang, *Nat. Metab.*, 2025, **7**, 421–433.
138 A. Pors, K. G. Rasmussen, R. Inglev, N. Jendrike, A. Philipps, A. G. Ranjan, V. Vestergaard, J. E. Henriksen, K. Nørgaard, G. Freckmann, K. D. Hepp, M. C. Gerstenberg and A. Weber, *ACS Sens.*, 2023, **8**, 1272–1279.
139 W. Liu, T. Han, W. Chen, J. Chen, Q. Ge, D. Sun, J. Liu and K. Xu, *Sensors*, 2025, **25**, 998.
140 U. Mogera, H. Guo, M. Namkoong, M. S. Rahman, T. Nguyen and L. Tian, *Sci. Adv.*, 2022, **8**, 1736.
141 X. He, C. Fan, Y. Luo, T. Xu and X. Zhang, *npj Flexible Electron.*, 2022, **6**, 60.
142 K. Yang, Z. Wang, K. Zhu, Y. Zhao, L. Wu, S. Zong and Z. Wang, *Talanta*, 2025, **293**, 128039.
143 X. Luo, Q. Yu, Y. Liu, W. Gai, L. Ye, L. Yang and Y. Cui, *ACS Sens.*, 2022, **7**, 1347–1360.
144 G. Bolat, E. De la Paz, N. F. Azeredo, M. Kartolo, J. Kim, A. N. de Loyola e Silva, R. Rueda, C. Brown, L. Angnes, J. Wang and J. R. Sempionatto, *Anal. Bioanal. Chem.*, 2022, **414**, 5411–5421.
145 B. Fan, Y. Wu, H. Guo, F. Yu, L.-E. Liu, S. Yu, J. Wang and Y. Wang, *Anal. Chim. Acta*, 2024, **1316**, 342852.
146 M. Li, L. Wang, R. Liu, J. Li, Q. Zhang, G. Shi, Y. Li, C. Hou and H. Wang, *Biosens. Bioelectron.*, 2021, **174**, 112828.
147 Y. Yang, C. Sheng, F. Dong and S. Liu, *Biosens. Bioelectron.*, 2024, **256**, 116280.
148 Y. Zhang, Z. Yang, C. Qiao, Y. Liu, C. Wang, X. Zeng, J. Hou, D. Huo and C. Hou, *Biosens. Bioelectron.*, 2024, **258**, 116354.
149 X. Yang, F. Wu, H. Huang, G. Zheng, H. Zhang, W. Cai, J. Li, Z.-Z. Yin and Y. Kong, *Biosens. Bioelectron.*, 2025, **272**, 117138.
150 W. Gao, X. Zhou, N. F. Heinig, J. P. Thomas, L. Zhang and K. T. Leung, *ACS Appl. Nano Mater.*, 2021, **4**, 4790–4799.
151 N. Promphet, C. Thanawattano, C. Buekban, T. Laochai, P. Lormaneenopparat, W. Sukmas, P. Rattanawaleedirojn, P. Puthongkham, P. Potiyaraj, W. Leewattanakit and N. Rodthongkum, *Anal. Chim. Acta*, 2024, **1312**, 342761.
152 C.-A. Vu, W.-W. Yang, H. W.-H. Chan and W.-Y. Chen, *Microchem. J.*, 2024, **207**, 112245.
153 G. Vulpe, G. Liu, S. Oakley, G. Yang, A. Ajith Mohan, M. Waldron and S. Sharma, *Lab Chip*, 2024, **24**, 2039–2048.
154 Y. Pan, M. He, J. Wu, H. Qi and Y. Cheng, *Sens. Actuators, B*, 2024, **401**, 135055.
155 H. Chenani, Z. Razaghi, M. Saeidi, A. H. Aghaii, M. A. Rastkhiz, M. Orouji, A. Ekrami and A. Simchi, *Talanta*, 2025, **287**, 127640.
156 Z. Wang, X. Bi, L. Tang, H. Sun, Z. Cao and C. Jiang, *Sens. Actuators, B*, 2025, **432**, 137506.
157 G. Li, C. Wang, Y. Chen, F. Liu, H. Fan, B. Yao, J. Hao, Y. Yu and D. Wen, *Small*, 2023, **19**, 2206868.
158 S. H. Tawakey, M. Mansour, A. Soltan and A. I. Salim, *Lab Chip*, 2024, **24**, 3958–3972.
159 J. Yang, X. Gong, S. Chen, Y. Zheng, L. Peng, B. Liu, Z. Chen, X. Xie, C. Yi and L. Jiang, *ACS Sens.*, 2023, **8**, 1241–1251.
160 Y. Liu, Q. Yu, L. Ye, L. Yang and Y. Cui, *Lab Chip*, 2023, **23**, 421–436.
161 Y. Liu, L. Yang and Y. Cui, *Microsyst. Nanoeng.*, 2024, **10**, 112.
162 Y. Chen, Y. Sun, Y. Li, Z. Wen, X. Peng, Y. He, Y. Hou, J. Fan, G. Zang and Y. Zhang, *Talanta*, 2024, **278**, 126499.
163 C. Chen, Y. Fu, S. S. Sparks, Z. Lyu, A. Pradhan, S. Ding, N. Boddeti, Y. Liu, Y. Lin, D. Du and K. Qiu, *ACS Sens.*, 2024, **9**, 3212–3223.
164 S. He, H. Lian, X. Cao, B. Liu and X. Wei, *Sens. Actuators, B*, 2022, **369**, 132345.
165 X. Liang, S. Zhang, S. Meng, R. Tan, K. Zhang and J. Hu, *Microchem. J.*, 2024, **207**, 111690.
166 R. Moreddu, V. Nasrollahi, P. Kassanos, S. Dimov, D. Vigolo and A. K. Yetisen, *Small*, 2021, **17**, 2102008.
167 Y. Bi, M. Sun, J. Wang, Z. Zhu, J. Bai, M. Y. Emran, A. Kotb, X. Bo and M. Zhou, *Anal. Chem.*, 2023, **95**, 6690–6699.
168 C. Yang, T. Sheng, W. Hou, J. Zhang, L. Cheng, H. Wang, W. Liu, S. Wang, X. Yu, Y. Zhang, J. Yu and Z. Gu, *Sci. Adv.*, 2022, **8**, eadd3197.
169 K. Mahato, T. Saha, S. Ding, S. S. Sandhu, A.-Y. Chang and J. Wang, *Nat. Electron.*, 2024, **7**, 735–750.
170 Y. Cheng, S. Feng, Q. Ning, T. Li, H. Xu, Q. Sun, D. Cui and K. Wang, *Microsyst. Nanoeng.*, 2023, **9**, 36.
171 J. Tu, J. Min, Y. Song, C. Xu, J. Li, J. Moore, J. Hanson, E. Hu, T. Parimon, T.-Y. Wang, E. Davoodi, T.-F. Chou, P. Chen, J. J. Hsu, H. B. Rossiter and W. Gao, *Nat. Biomed. Eng.*, 2023, 1293–1306.
172 C. Huang, D. Li, J. Liu, S. Hou, W. Yang, H. Wang, J. Wang, Z. Wang, F. Li, Z. Hao, S. Huang, X. Zhao, P. Hu and Y. Pan, *Adv. Funct. Mater.*, 2023, **34**, 2309447.
173 M. Ploner, B. Shkodra, L. Franchin, A. Altana, M. Petrelli, M. A. Costa Angeli, G. Ciccone, T. Antrack, L. Vanzetti, R. R. Nair, R. Canteri, S. Bonaldo, A. Paccagnella, H. Kleemann, D. Resnati, P. Lugli, A. Erten and L. Petti, *Biosens. Bioelectron.*, 2025, **287**, 117734.
174 H. Chu, X. Hu, C.-Y. Lee, A. Zhang, Y. Ye, Y. Wang, Y. Chen, X. Yan, X. Wang, J. Wei, S. He and Y. Li, *Biosens. Bioelectron.*, 2023, **232**, 115301.
175 J. Fu, Y. Wang, Y. Ding, J. Wang, S. Deng, Z. Jiang, C. S. Tan and S. Li, *Talanta*, 2025, **287**, 127608.
176 Z. Wang, Z. Hao, S. Yu, C. G. De Moraes, L. H. Suh, X. Zhao and Q. Lin, *Adv. Funct. Mater.*, 2019, **29**, 1905202.
177 Z. Hao, Y. Luo, C. Huang, Z. Wang, G. Song, Y. Pan, X. Zhao and S. Liu, *Small*, 2021, **17**, 2101508.
178 C. Huang, W. Yang, H. Wang, S. Huang, S. Gao, D. Li, J. Liu, S. Hou, W. Feng, Z. Wang, F. Li, Z. Hao, X. Zhao, P. Hu and Y. Pan, *ACS Nano*, 2024, **18**, 21198–21210.
179 C. Huang, W. Feng, S. Hou, Z. Jiang, Y. Wu, Y. Wang, D. Ding, S. Gao, F. Li, X. Zhao, P. Hu and Y. Pan, *Chem. Eng. J.*, 2025, **520**, 165940.
180 Z. Wang, Z. Hao, X. Wang, C. Huang, Q. Lin, X. Zhao and Y. Pan, *Adv. Funct. Mater.*, 2021, **31**, 2005958.
181 B. Q. Tran, P. R. Miller, R. M. Taylor, G. Boyd, P. M. Mach, C. N. Rosenzweig, J. T. Baca, R. Polsky and T. Glaros, *J. Proteome Res.*, 2018, **17**, 479–485.

182 M. Dervisevic, M. Alba, T. E. Adams, B. Prieto-Simon and N. H. Voelcker, *Biosens. Bioelectron.*, 2021, **192**, 113496.
183 D. Oliveira, B. P. Correia, S. Sharma and F. T. C. Moreira, *ACS Omega*, 2022, **7**, 39039–39044.
184 J. Xu, B. Yang, J. Kong, Y. Zhang and X. Fang, *Adv. Healthcare Mater.*, 2023, **12**, 2203133.
185 W. L. Stuard, R. Titone and D. M. Robertson, *Eye Contact Lens*, 2020, **46**, 319–325.
186 M. Sheikhrezaee, M. R. Alizadeh and S. Abediankenari, *Int. J. Diabetes Dev. Ctries.*, 2020, **40**, 93–98.
187 Y.-C. Wu, B. R. Buckner, M. Zhu, H. D. Cavanagh and D. M. Robertson, *Ocul. Surf.*, 2012, **10**, 100–107.
188 F. Fan, X. Li, K. Li and Z. Jia, *Ther. Clin. Risk Manage.*, 2021, **17**, 797–807.
189 K. Sampani, S. Ness, F. Tuz-Zahra, N. Aytan, E. E. Spurlock, S. Alluri, X. Chen, N. H. Siegel, M. L. Alosco, W. Xia, Y. Tripodis, T. D. Stein and M. L. Subramanian, *Alzheimers Res. Ther.*, 2024, **16**, 192.
190 N. Van De Sande, I. H. G. B. Ramakers, P. J. Visser, F. R. J. Verhey, F. D. Verbraak, F. H. Bouwman, T. T. J. M. Berendschot, R. M. M. A. Nuijts, C. A. B. Webers and M. Gijs, *BMC Neurol.*, 2023, **23**, 293.
191 S. E. Woo and S. Y. Jang, *Semin. Ophthalmol.*, 2021, **36**, 128–131.
192 J. Jang, J. Kim, H. Shin, Y.-G. Park, B. J. Joo, H. Seo, J.-E. Won, D. W. Kim, C. Y. Lee, H. K. Kim and J.-U. Park, *Sci. Adv.*, 2021, **7**, eabf7194.
193 J. Xu, X. Tao, X. Liu and L. Yang, *Anal. Chem.*, 2022, **94**, 8659–8667.
194 A. Manjeri and S. D. George, *Lab Chip*, 2024, **24**, 2327–2334.
195 S. Upasham, P. Rice, M. Pali and S. Prasad, *Biosens. Bioelectron.: X*, 2022, **10**, 100120.
196 H. Guan, T. Zhong, H. He, T. Zhao, L. Xing, Y. Zhang and X. Xue, *Nano Energy*, 2019, **59**, 754–761.
197 B. Jagannath, K. C. Lin, M. Pali, D. Sankhala, S. Muthukumar and S. Prasad, *Bioeng. Transl. Med.*, 2021, **6**, 10220.
198 Z. Hao, Z. Wang, Y. Li, Y. Zhu, X. Wang, C. G. De Moraes, Y. Pan, X. Zhao and Q. Lin, *Nanoscale*, 2018, **10**, 21681–21688.
199 E. C. Wilkirson, D. Li and P. B. Lillehoj, *ACS Sens.*, 2024, **9**, 5792–5801.
200 L. Dosnon, T. Rduch, C. Meyer and I. K. Herrmann, *Adv. Sci.*, 2025, 05170.
201 T. A. Feagin, N. Maganzini and H. T. Soh, *ACS Sens.*, 2018, **3**, 1611–1615.
202 M. Santos-Cancel, R. A. Lazenby and R. J. White, *ACS Sens.*, 2018, **3**, 1203–1209.
203 Z. Zhang, P. Sen, B. R. Adhikari, Y. Li and L. Soleymani, *Angew. Chem., Int. Ed.*, 2022, **61**, e202212496.
204 C. Ye, H. Lukas, M. Wang, Y. Lee and W. Gao, *Chem. Soc. Rev.*, 2024, **53**, 7960–7982.
205 G. C. Biswas, M. T. M. Khan and J. Das, *Biosens. Bioelectron.*, 2023, **226**, 115115.
206 H. Yousefi, A. Mahmud, D. Chang, J. Das, S. Gomis, J. B. Chen, H. Wang, T. Been, L. Yip, E. Coomes, Z. Li, S. Mubareka, A. McGeer, N. Christie, S. Gray-Owen, A. Cochrane, J. M. Rini, E. H. Sargent and S. O. Kelley, *J. Am. Chem. Soc.*, 2021, **143**, 1722–1727.
207 Z. Zhang, R. Pandey, J. Li, J. Gu, D. White, H. D. Stacey, J. C. Ang, C.-J. Steinberg, A. Capretta, C. D. M. Filipe, K. Mossman, C. Balion, M. S. Miller, B. J. Salena, D. Yamamura, L. Soleymani, J. D. Brennan and Y. Li, *Angew. Chem., Int. Ed.*, 2021, **60**, 24266–24274.
208 A. Victorious, Z. Zhang, D. Chang, R. Maclachlan, R. Pandey, J. Xia, J. Gu, T. Hoare, L. Soleymani and Y. Li, *Angew. Chem., Int. Ed.*, 2022, **61**, e202204252.
209 P. Q. Nguyen, L. R. Soenksen, N. M. Donghia, N. M. Angenent-Mari, H. De Puig, A. Huang, R. Lee, S. Slomovic, T. Galbersanini, G. Lansberry, H. M. Sallum, E. M. Zhao, J. B. Niemi and J. J. Collins, *Nat. Biotechnol.*, 2021, **39**, 1366–1374.
210 B. Yang, J. Kong and X. Fang, *Nat. Commun.*, 2022, **13**, 3999.
211 M. Kong, Z. Li, J. Wu, J. Hu, Y. Sheng, D. Wu, Y. Lin, M. Li, X. Wang and S. Wang, *Talanta*, 2019, **205**, 120155.
212 B. Yang, J. Kong and X. Fang, *Talanta*, 2019, **204**, 685–692.
213 H. E. Kim, A. Schuck, S. H. Lee, Y. Lee, M. Kang and Y.-S. Kim, *Biosens. Bioelectron.*, 2021, **182**, 113168.
214 W. Xu, T. Jin, Y. Dai and C. C. Liu, *Biosens. Bioelectron.*, 2020, **155**, 112100.
215 C. Shi, D. Yang, X. Ma, L. Pan, Y. Shao, G. Arya, Y. Ke, C. Zhang, F. Wang, X. Zuo, M. Li and P. Wang, *Angew. Chem., Int. Ed.*, 2024, **63**, 202320179.
216 A. Suea-Ngam, P. D. Howes and A. J. deMello, *Chem. Sci.*, 2021, **12**, 12733–12743.
217 Dexcom G7 CGM System, https://www.dexcom.com/en-us/g7-cgm-system, (accessed January 2026).
218 Guardian Sensor 4, https://www.medtronicdiabetes.com/products/guardian-sensor-4, (accessed January 2026).
219 Guardian Connect Continuous Glucose Monitoring System, https://www.medtronicdiabetes.com/products/guardian-connect-continuous-glucose-monitoring-system, (accessed January 2026).
220 FreeStyle Libre 3 System, https://www.freestyle.abbott/us-en/products/freestyle-libre-3.html, (accessed January 2026).
221 L. B. Baker, J. B. Model, K. A. Barnes, M. L. Anderson, S. P. Lee, K. A. Lee, S. D. Brown, A. J. Reimel, T. J. Roberts, R. P. Nuccio, J. L. Bonsignore, C. T. Ungaro, J. M. Carter, W. Li, M. S. Seib, J. T. Reeder, A. J. Aranyosi, J. A. Rogers and R. Ghaffari, *Sci. Adv.*, 2020, **6**, eabe3929.
222 L. B. Baker, M. S. Seib, K. A. Barnes, S. D. Brown, M. A. King, P. J. D. De Chavez, S. Qu, J. Archer, A. S. Wolfe, J. R. Stofan, J. M. Carter, D. E. Wright, J. Wallace, D. S. Yang, S. Liu, J. Anderson, T. Fort, W. Li, J. A. Wright, S. P. Lee, J. B. Model, J. A. Rogers, A. J. Aranyosi and R. Ghaffari, *Adv. Mater. Technol.*, 2022, **7**, 2200249.

